



CHAPTER 8

**The role of neuroinflammation
pathomechanism on autism
spectrum disorder and unraveling
potential biomarkers for early
detection**

The role of neuroinflammation pathomechanism on autism spectrum disorder and unraveling potential biomarkers for early detection

8.1. Abstract

Autism spectrum disorder (ASD) is a complex neurological and developmental condition characterized by a broad range of symptoms. Numerous studies have implicated multi-genetic and epigenetic factors in the etiology of ASD, and efforts have been made to identify potential biomarkers. However, the quest for potent and precise biomarkers for the detection and diagnosis of ASD remains an unmet challenge. In this study, a comprehensive bioinformatic analysis of gene expression profiles from ASD patients was conducted to identify common genes that serve as potential and reliable biomarkers for early diagnosis of ASD, particularly from accessible tissues. The analysis of brain datasets revealed 581 differentially expressed genes (DEGs), with functional enrichment implicating processes such as positive regulation of cytokine production, response to bacterial molecules, and involvement in the TNF signaling pathway.

In contrast, the blood dataset exhibited sixty significant DEGs associated with inflammatory responses, including chemokine response and the interaction of cytokines and cytokine receptors. Remarkably, eight common genes were identified between the two datasets. Among these common DEGs, *UPBI*, *CXCL1*, *CXCL10*, *CSF1*, *CCL2*, and *IL1B* were identified as novel genes associated with ASD, while *FFAR2* and *WWC2-AS2* were novel genes not previously linked to ASD. The common genes were enriched in the TNF signaling pathway. The findings revealed the relevance of immunity dysregulation in the neurodevelopmental of ASD. Additionally, these common genes hold promise as prospective biomarkers for early detection from accessible tissues and represent potential targets for future pharmacological interventions in ASD.

8.2. Introduction

Autism spectrum disorder (ASD) is a category of neurodevelopmental diseases that influence the development of neurological pathways, presenting a diverse array of manifestations, including impairment in communication, stereotypical behavior patterns, speech troubles, and social interaction deficits [1]. ASD has been exhibited an

imbalanced gender distribution, with boys showing a fourfold higher susceptibility than girls [2].

Heterogeneity and diversity in manifestations of ASD support the complex genetic and environmental etiology of ASD [3]. One of the largest studies to date, including more than two million children, concluded that 45–56% of ASD are inheritable [4]. Multiple studies have identified both frequent and rare variants, revealing the complexity of ASD disorder [5-7]. Moreover, accumulating studies have supported the involvement of numerous genetic variations in synaptopathies and neuroinflammation as pathomechanisms in ASD [8-10]. Than and his colleagues analyzed the composition of cerebrospinal fluid (CSF), and their findings revealed elevated levels of four inflammatory cytokines (TNF- α , IL-4, and IL-21) that play fundamental roles as inflammatory mediators driving the neuro-immune system in ASD patients [11]. In the same context, an investigation of the whole blood for detecting markers revealed three genes, namely *NMUR1*, *HMGB3*, and *PTPRN2*, were differently expressed and associated with ASD. Subsequent analysis of their ASD-associated signature highlighted the dysregulation of immune-inflammatory pathways [12]. Meta-analysis of postmortem brain tissue demonstrated 235 new differentially expressed genes (DEGs) not detected in previous studies. Gene ontology (GO) enrichment analysis identified the upregulation of genes involved in inflammatory immune response pathways, including TNF signaling [13]. In the same context, samples from Whole-exome sequence data of approximately 35,584, including 11,986 with ASD, were analyzed. It found 102 genes implicated in ASD risk, and 30 novel critical genes were reported [7].

Even though numerous studies have been conducted to define gene expression alterations from brain tissues in ASD, they have successfully predicted cellular and molecular processes that might have critical roles in the neurological development of ASD [6, 13-15]. Nevertheless, the genes may not possess predictive value if they are not expressed or modified in accessible tissues. Conversely, many high-risk genes were detected in various obtainable tissues, such as blood [12], saliva [16], and placenta [14], without confirming their crucial roles in the brain of ASD patients. Therefore, in the current study, two datasets from peripheral blood and post-mortem brain (PMB) tissue transcriptomes of ASD samples were used to identify the common genes as susceptible biomarkers for ASD diagnosis using accessible tissue. In this regard, DEGs and

functional enrichment analyses were performed separately to determine the top robust DEGs, GO, and biological pathways for each dataset to shed light on the putative processes underlying the etiology of ASD. Additionally, the overlap between studied DEGs lists was carried out to identify the common genes and their molecular biological pathways enriched within as candidate biomarkers with the benefits of early diagnosis in a consistent and reliable pathogenesis which may facilitate diagnostic precisions and therapeutic opinions.

8.3. Material and methodology

8.3.1. Acquisition of the transcriptomic Datasets

A transcriptomic database acquired RNA-Seq datasets of human ASD patients from Gene Expression Omnibus (GEO). The datasets were obtained from the GSE178205 dataset of frozen human brain samples [17] and GSE64018 [18], consisting of 47 samples (25 ASD, 22 typically developing control (TD)).

Furthermore, the subgroup dataset was nominated from the GSE140702 dataset of cultured peripheral blood monocyte samples [19]. This subgroup included TD control children (N = 23) (19 male, 4 female) and ASD patients (N = 25) (autism disorder AD (13 male, 4 female), Pervasive Developmental Disorder- Not Otherwise Specified(PDD-NOS) patients (6 male, 2 female)).

8.3.2. Differentially expressed genes analysis of two datasets

DESeq2 package [20] was applied to determine differentially expressed genes when comparing control versus ASD samples within the two datasets. Filtering criteria were implemented to identify statistically significant genes in the brain and blood datasets separately, employing P -value < 0.01 and $-1 > \log_2\text{FoldChange} > 1$ to mark upregulated and downregulated genes.

8.3.3. Functional annotation analysis

8.3.3.1. Gene ontology and enriched pathway analysis

Gene over-representation analysis was carried out independently on the two datasets using the ClusterProfiler R package [21] to identify cellular components (CC), biological processes (BP), and molecular functions (MF). Enrichment for Gene Ontology (GO) terms and pathways was determined based on a significance threshold of P -value < 0.01 .

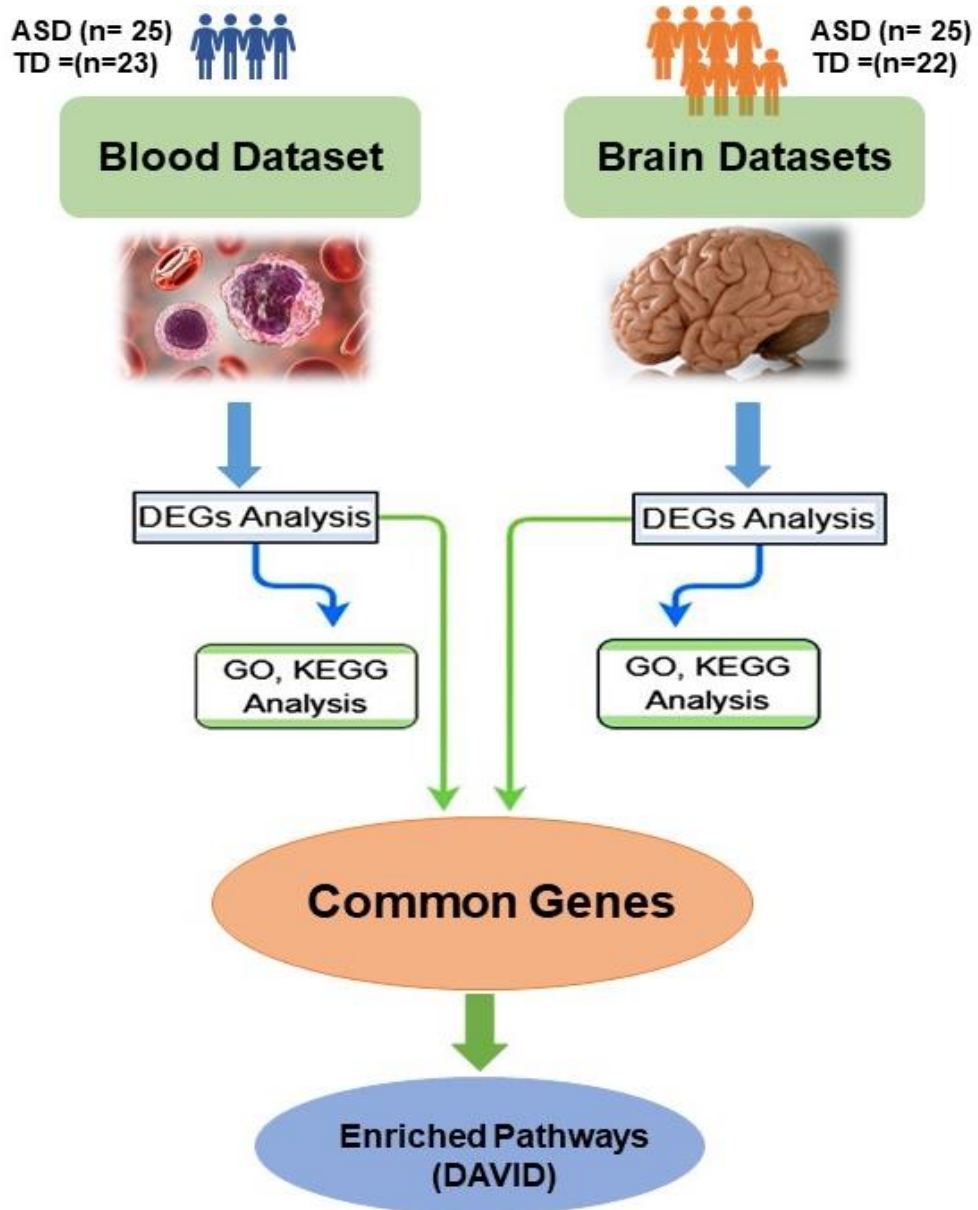
Additionally, the Kyoto Encyclopedia of Genes and Genomes (KEGG) analysis was performed using the ClusterProfiler package.

8.3.4. Comparison of the DEGs between the two datasets in silico

Utilizing a Venn diagram, common DEGs between differentially expressed genes from the PMB tissue datasets and DEGs from the blood dataset were identified, taking into account a significance threshold of P -value < 0.01 . ClusterProfiler R package was applied.

8.3.5. The Database for Annotation, Visualization, and Integrated Discovery (DAVID)

A functional profile was constructed by employing genes that exhibited differential expression in both datasets through the DAVID server. The meta-analysis workflow conducted to identify common differentially expressed genes is illustrated in (**Scheme 8.1**).



Scheme 8.1 The flowchart shows the meta-analysis workflow. ASD: autism spectrum disorder, TD: typically developing, DEGs: differentially expressed genes, GO: gene ontology, KEGG: kyoto encyclopedia of genes and genomes, DAVID: database for annotation, visualization, and integrated Discovery.

8.4. Results

8.4.1. Identification of DEGs

The comprehensive analysis of differential expression revealed a total of 581 DEGs in the ASD brain dataset, meeting the criteria of P -value < 0.01 (Table 8.1). Among these, 520 genes exhibited significant upregulation with cut-off $\text{Log}_2\text{FC} > 1$, whereas 61 genes displayed downregulation with cut-off $\text{Log}_2\text{FC} < -1$ (Figure 8.1A). Hierarchical clustering analysis underscored a distinct DEGs profile, highlighting the notable differences between ASD patients and control subjects. In the blood dataset analysis, significant DEGs between ASD and typically developing controls were identified using the P -value < 0.01 and $1 < \text{Log}_2\text{FC} < -1$ criteria, resulting in a curated list of 60 genes. Notably, six of these genes were novel namely (*SYNPO2*, *WWC2-AS2*, *CNIH3*, *RN7SL239P*, *KRT86*, and *TRIB3*) (Table 8.2) with 20 genes downregulated and 40 genes upregulated. The volcano plot represented the DEGs in (Figure 8.1B).

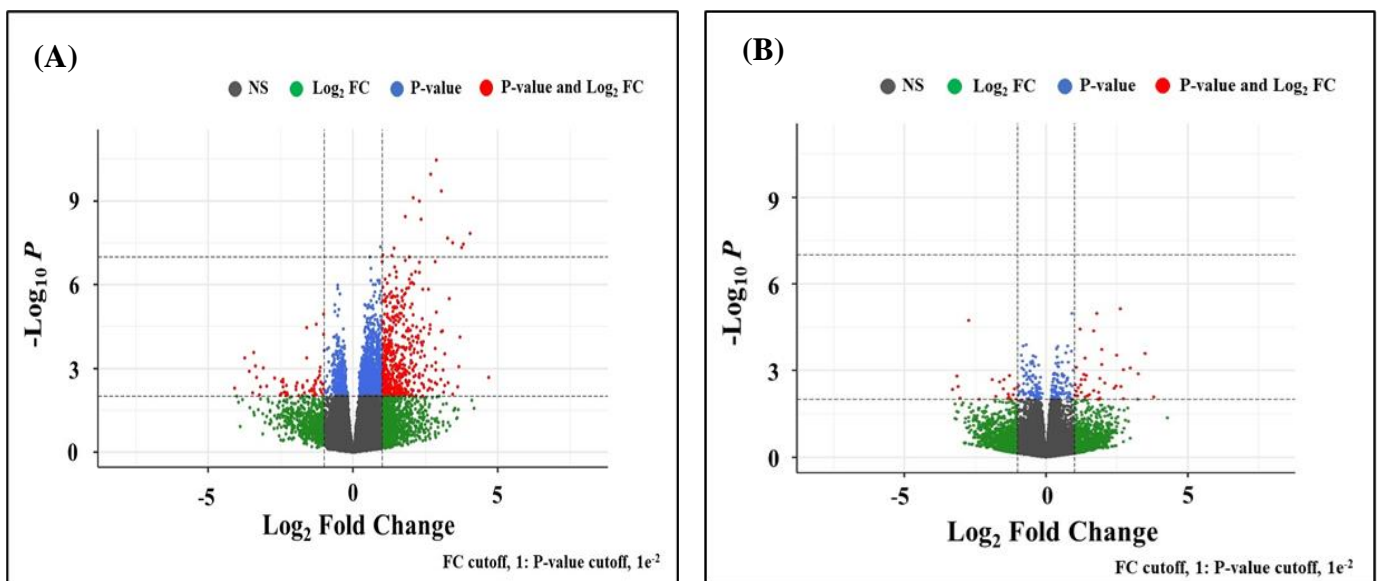


Figure 8.1. Differential expression genes using the Volcano plot. (A) The brain datasets show 581 significant genes (P -value < 0.01 and $1 < \text{Log}_2\text{FC} < -1$ as thresholds) in red dots left. **(B)** The blood monocytes dataset showed 60 DEGs in red dots.

Table 8.1. The differential expressed genes DEGs of brain datasets (-1 >Log2FoldChange > 1, *P*-value < 0.01)

| Symbol | Entrez Gene ID | log2FoldChange | <i>P</i>-value | <i>P</i>-adj |
|------------------|---------------------------|-----------------------|-----------------------|---------------------|
| <i>HSPA6</i> | 3310 | 5.761707 | 5.87E-14 | 1.21E-09 |
| <i>HSPB1</i> | 3315 | 2.746181 | 8.49E-13 | 5.45E-09 |
| <i>SERPINH1</i> | 871 | 3.279011 | 1.06E-12 | 5.45E-09 |
| <i>BAG3</i> | 9531 | 2.892517 | 5.47E-13 | 5.45E-09 |
| <i>HSPA1A</i> | 3303 | 2.875769 | 3.50E-11 | 1.45E-07 |
| <i>HMOX1</i> | 3162 | 2.688162 | 1.13E-10 | 3.89E-07 |
| <i>RRAD</i> | 6236 | 3.046311 | 4.46E-10 | 1.31E-06 |
| <i>DEPPI</i> | 11067 | 2.070287 | 7.74E-10 | 2.00E-06 |
| <i>DNAJB1</i> | 3337 | 2.285098 | 1.05E-09 | 2.40E-06 |
| <i>NFKB2</i> | 4791 | 1.799041 | 3.70E-09 | 7.63E-06 |
| <i>CDKN1A</i> | 1026 | 2.353722 | 4.50E-09 | 8.45E-06 |
| <i>CSF3</i> | 1440 | 4.037722 | 1.48E-08 | 2.54E-05 |
| <i>SOCS3</i> | 9021 | 3.27043 | 2.17E-08 | 3.44E-05 |
| <i>NPAS4</i> | 266743 | 3.431592 | 3.11E-08 | 4.59E-05 |
| <i>SERPINA3</i> | 12 | 3.809963 | 3.57E-08 | 4.91E-05 |
| <i>LINC02138</i> | 400558 | 3.75165 | 4.61E-08 | 5.60E-05 |
| <i>BST2</i> | 684 | 1.411501 | 4.95E-08 | 5.68E-05 |
| <i>CSF1</i> | 1435 | 1.340807 | 9.09E-08 | 9.38E-05 |
| <i>ZC3HAV1</i> | 56829 | 1.01853 | 8.82E-08 | 9.38E-05 |
| <i>MAFF</i> | 23764 | 1.939069 | 1.02E-07 | 9.82E-05 |
| <i>CCNI</i> | 3491 | 1.810254 | 1.33E-07 | 0.00012 |
| <i>MKNK2</i> | 2872 | 1.015318 | 1.48E-07 | 0.000126 |
| <i>TNFRSF12A</i> | 51330 | 2.845228 | 1.53E-07 | 0.000126 |
| <i>GADD45B</i> | 4616 | 2.299832 | 1.63E-07 | 0.00013 |
| <i>CEBPD</i> | 1052 | 1.440674 | 2.38E-07 | 0.000182 |
| <i>FPR1</i> | 2357 | 2.152125 | 3.55E-07 | 0.000243 |
| <i>PPP1R15A</i> | 23645 | 1.489687 | 3.45E-07 | 0.000243 |
| <i>GBP1</i> | 2633 | 2.289502 | 3.64E-07 | 0.000243 |

| | | | | |
|-----------------|--------|----------|----------|----------|
| <i>SPHK1</i> | 8877 | 2.020066 | 4.32E-07 | 0.000279 |
| <i>HAPI</i> | 9001 | 1.263774 | 4.64E-07 | 0.00029 |
| <i>GADD45G</i> | 10912 | 1.503308 | 5.32E-07 | 0.000323 |
| <i>EIF4EBP1</i> | 1978 | 1.101979 | 6.34E-07 | 0.000373 |
| <i>FOSB</i> | 2354 | 1.946419 | 6.50E-07 | 0.000373 |
| <i>GBP2</i> | 2634 | 2.032393 | 8.37E-07 | 0.000432 |
| <i>ICAM1</i> | 3383 | 1.977718 | 8.97E-07 | 0.000434 |
| <i>SPI1</i> | 6688 | 1.190007 | 8.80E-07 | 0.000434 |
| <i>INHBA</i> | 3624 | 2.099578 | 9.60E-07 | 0.00045 |
| <i>CHI3L1</i> | 1116 | 1.925294 | 1.29E-06 | 0.000531 |
| <i>MSN</i> | 4478 | 1.029658 | 1.24E-06 | 0.000531 |
| <i>VASP</i> | 7408 | 1.022996 | 1.28E-06 | 0.000531 |
| <i>TNFAIP3</i> | 7128 | 1.501024 | 1.36E-06 | 0.000541 |
| <i>CD14</i> | 929 | 1.840842 | 1.36E-06 | 0.000541 |
| <i>SPP1</i> | 6696 | 2.595834 | 1.43E-06 | 0.000547 |
| <i>CD44</i> | 960 | 2.414603 | 1.46E-06 | 0.000547 |
| <i>TYMP</i> | 1890 | 1.698211 | 1.65E-06 | 0.000609 |
| <i>IRF1</i> | 3659 | 1.328726 | 1.81E-06 | 0.000643 |
| <i>C5AR1</i> | 728 | 1.807005 | 2.10E-06 | 0.000719 |
| <i>RHBDF2</i> | 79651 | 1.254428 | 2.14E-06 | 0.000719 |
| <i>FOS</i> | 2353 | 1.764481 | 2.26E-06 | 0.00074 |
| <i>PIM1</i> | 5292 | 1.080763 | 2.34E-06 | 0.000755 |
| <i>FAM166C</i> | 339778 | 1.539864 | 2.54E-06 | 0.000781 |
| <i>OAS3</i> | 4940 | 1.372264 | 2.50E-06 | 0.000781 |
| <i>DDIT4</i> | 54541 | 1.186545 | 2.68E-06 | 0.000801 |
| <i>NUPRI</i> | 26471 | 1.460617 | 2.74E-06 | 0.000808 |
| <i>NQO1</i> | 1728 | 1.328235 | 2.90E-06 | 0.000825 |
| <i>MX2</i> | 4600 | 1.356871 | 2.84E-06 | 0.000825 |
| <i>HELZ2</i> | 85441 | 1.687884 | 2.92E-06 | 0.000825 |
| <i>TNFRSF1A</i> | 7132 | 1.127309 | 3.17E-06 | 0.000884 |
| <i>SFN</i> | 2810 | 3.330597 | 3.23E-06 | 0.000888 |
| <i>ADM</i> | 133 | 1.711917 | 3.83E-06 | 0.000995 |

| | | | | |
|------------------|----------|----------|----------|----------|
| <i>PARP14</i> | 54625 | 1.116163 | 3.90E-06 | 0.000995 |
| <i>PYGL</i> | 5836 | 1.033585 | 3.74E-06 | 0.000995 |
| <i>CIQC</i> | 714 | 1.534452 | 3.81E-06 | 0.000995 |
| <i>PLSCRI</i> | 5359 | 1.089636 | 4.10E-06 | 0.001032 |
| <i>FERMT3</i> | 83706 | 1.576382 | 4.44E-06 | 0.001063 |
| <i>ATOH8</i> | 84913 | 1.274708 | 4.48E-06 | 0.001063 |
| <i>SLC16A3</i> | 9123 | 1.557673 | 4.43E-06 | 0.001063 |
| <i>HTRA3</i> | 94031 | 2.037349 | 5.03E-06 | 0.00118 |
| <i>CD93</i> | 22918 | 1.792218 | 5.16E-06 | 0.001184 |
| <i>PLIN2</i> | 123 | 1.16446 | 5.86E-06 | 0.001272 |
| <i>ATF3</i> | 467 | 1.676841 | 6.05E-06 | 0.001301 |
| <i>C11orf96</i> | 387763 | 1.43349 | 6.18E-06 | 0.001302 |
| <i>MMP14</i> | 4323 | 1.5091 | 6.63E-06 | 0.001355 |
| <i>SCIN</i> | 85477 | 1.982044 | 6.61E-06 | 0.001355 |
| <i>PLK5</i> | 126520 | 1.747492 | 6.90E-06 | 0.001356 |
| <i>HIC1</i> | 3090 | 1.439835 | 6.82E-06 | 0.001356 |
| <i>CHST3</i> | 9469 | 1.375813 | 6.73E-06 | 0.001356 |
| <i>TNFRSF1B</i> | 7133 | 1.379135 | 8.94E-06 | 0.001709 |
| <i>PELATON</i> | 1.01E+08 | 2.867703 | 9.49E-06 | 0.00178 |
| <i>PLAAT4</i> | 5920 | 1.613809 | 1.07E-05 | 0.001985 |
| <i>MIR3619</i> | 1.01E+08 | 1.669635 | 1.10E-05 | 0.002019 |
| <i>LINC02217</i> | 1.02E+08 | -1.01323 | 1.14E-05 | 0.002071 |
| <i>IFI16</i> | 3428 | 1.086368 | 1.14E-05 | 0.002071 |
| <i>DTX3L</i> | 151636 | 1.179406 | 1.17E-05 | 0.002108 |
| <i>OSGIN1</i> | 29948 | 1.512382 | 1.21E-05 | 0.002149 |
| <i>AMN</i> | 81693 | 2.072347 | 1.23E-05 | 0.002149 |
| <i>RDH10</i> | 157506 | 1.75251 | 1.33E-05 | 0.002293 |
| <i>GEM</i> | 2669 | 1.447218 | 1.37E-05 | 0.002297 |
| <i>PTPN6</i> | 5777 | 1.186311 | 1.40E-05 | 0.002297 |
| <i>THBD</i> | 7056 | 1.363866 | 1.40E-05 | 0.002297 |
| <i>KCNE4</i> | 23704 | 1.561336 | 1.44E-05 | 0.002345 |
| <i>JUNB</i> | 3726 | 1.234335 | 1.61E-05 | 0.002532 |

| | | | | |
|---------------------|----------|----------|----------|----------|
| <i>ADAMTS9</i> | 56999 | 1.387952 | 1.61E-05 | 0.002532 |
| <i>COL18A1</i> | 80781 | 1.248728 | 1.62E-05 | 0.002532 |
| <i>CXCL10</i> | 3627 | 2.387652 | 1.68E-05 | 0.002565 |
| <i>CIQB</i> | 713 | 1.621971 | 1.68E-05 | 0.002565 |
| <i>EPS8L1</i> | 54869 | 1.843859 | 1.85E-05 | 0.00275 |
| <i>NMB</i> | 4828 | 1.293399 | 1.87E-05 | 0.002752 |
| <i>PLAUR</i> | 5329 | 1.471298 | 1.92E-05 | 0.002787 |
| <i>ONECUT1</i> | 3175 | 1.57517 | 2.07E-05 | 0.002992 |
| <i>FLNA</i> | 2316 | 1.010096 | 2.13E-05 | 0.003056 |
| <i>SLC15A3</i> | 51296 | 1.044035 | 2.15E-05 | 0.003061 |
| <i>IFITM3</i> | 10410 | 1.390748 | 2.29E-05 | 0.003171 |
| <i>NES</i> | 10763 | 1.061736 | 2.47E-05 | 0.00335 |
| <i>MSR1</i> | 4481 | 1.747428 | 2.59E-05 | 0.003477 |
| <i>PVALB</i> | 5816 | -1.27382 | 2.69E-05 | 0.003563 |
| <i>LOC101929076</i> | 1.02E+08 | 2.66195 | 2.83E-05 | 0.003624 |
| <i>C4B</i> | 721 | 1.481683 | 2.78E-05 | 0.003624 |
| <i>LRRC32</i> | 2615 | 1.262908 | 3.06E-05 | 0.00383 |
| <i>SLC11A1</i> | 6556 | 2.066839 | 3.03E-05 | 0.00383 |
| <i>KISS1R</i> | 84634 | 2.191113 | 3.23E-05 | 0.003992 |
| <i>GABRA6</i> | 2559 | -1.58925 | 3.43E-05 | 0.004191 |
| <i>HSPA1B</i> | 3304 | 2.442323 | 3.48E-05 | 0.004225 |
| <i>THBS1</i> | 7057 | 1.349217 | 3.58E-05 | 0.004268 |
| <i>COL4A2</i> | 1284 | 1.010457 | 3.64E-05 | 0.004308 |
| <i>FOSL1</i> | 8061 | 1.902364 | 3.70E-05 | 0.004342 |
| <i>LINC01686</i> | 284648 | 2.652634 | 3.90E-05 | 0.004469 |
| <i>H2AC11</i> | 8969 | 1.353433 | 3.96E-05 | 0.004513 |
| <i>PDLIM4</i> | 8572 | 1.247213 | 4.01E-05 | 0.004524 |
| <i>KCTD11</i> | 147040 | 1.119401 | 4.08E-05 | 0.004552 |
| <i>YBX3</i> | 8531 | 1.288823 | 4.11E-05 | 0.004556 |
| <i>ARID5A</i> | 10865 | 1.101296 | 4.21E-05 | 0.004643 |
| <i>ATP8B3</i> | 148229 | 1.978929 | 4.38E-05 | 0.004731 |
| <i>LGALS9</i> | 3965 | 1.345381 | 4.52E-05 | 0.004809 |

| | | | | |
|------------------|----------|----------|----------|----------|
| <i>RDH10-AS1</i> | 1.02E+08 | 1.911925 | 4.58E-05 | 0.004851 |
| <i>FSCN2</i> | 25794 | 1.836721 | 4.62E-05 | 0.004869 |
| <i>ADGRG3</i> | 222487 | 2.332311 | 4.71E-05 | 0.004935 |
| <i>AEBPI</i> | 165 | 1.173331 | 4.82E-05 | 0.004948 |
| <i>FLNC</i> | 2318 | 1.184242 | 4.81E-05 | 0.004948 |
| <i>LCPI</i> | 3936 | 1.172683 | 4.85E-05 | 0.00495 |
| <i>RNF223</i> | 401934 | 3.053645 | 4.87E-05 | 0.00495 |
| <i>GJA4</i> | 2701 | 1.085325 | 5.04E-05 | 0.005073 |
| <i>S100A11</i> | 6282 | 1.486716 | 5.09E-05 | 0.005083 |
| <i>CHI3L2</i> | 1117 | 2.61392 | 5.77E-05 | 0.005562 |
| <i>FLT3</i> | 2322 | -1.01402 | 6.23E-05 | 0.005869 |
| <i>APOL6</i> | 80830 | 1.279393 | 6.21E-05 | 0.005869 |
| <i>STUB1-DT</i> | 1.05E+08 | 2.260003 | 6.69E-05 | 0.006167 |
| <i>NGFR</i> | 4804 | 1.734427 | 6.91E-05 | 0.006283 |
| <i>APOL1</i> | 8542 | 1.257136 | 6.90E-05 | 0.006283 |
| <i>CD163</i> | 9332 | 2.030501 | 7.02E-05 | 0.006348 |
| <i>APOBR</i> | 55911 | 1.701579 | 7.17E-05 | 0.006437 |
| <i>MIR4525</i> | 1.01E+08 | 2.183198 | 7.41E-05 | 0.006532 |
| <i>PTGER1</i> | 5731 | 1.795517 | 7.51E-05 | 0.006542 |
| <i>PXN</i> | 5829 | 1.124314 | 7.46E-05 | 0.006542 |
| <i>KDM6B</i> | 23135 | 1.036946 | 8.64E-05 | 0.007133 |
| <i>RGS1</i> | 5996 | 2.247389 | 8.64E-05 | 0.007133 |
| <i>COX6B2</i> | 125965 | 1.918802 | 8.73E-05 | 0.007147 |
| <i>CXCL2</i> | 2920 | 1.893837 | 9.06E-05 | 0.007364 |
| <i>STAB1</i> | 23166 | 1.214234 | 9.44E-05 | 0.007527 |
| <i>MYC</i> | 4609 | 1.110292 | 9.95E-05 | 0.007807 |
| <i>GLI2</i> | 2736 | 1.318774 | 0.000101 | 0.007926 |
| <i>S100A10</i> | 6281 | 1.269785 | 0.000105 | 0.008108 |
| <i>PRKAG3</i> | 53632 | 2.078557 | 0.000108 | 0.008293 |
| <i>MT2A</i> | 4502 | 1.267522 | 0.00011 | 0.008338 |
| <i>GPR25</i> | 2848 | 2.424925 | 0.000111 | 0.008348 |
| <i>NKX2-8</i> | 26257 | 2.347817 | 0.000116 | 0.008632 |

| | | | | |
|-------------------|----------|----------|----------|----------|
| <i>CD164L2</i> | 388611 | 2.223197 | 0.000121 | 0.008923 |
| <i>SECTM1</i> | 6398 | 1.955898 | 0.000122 | 0.008946 |
| <i>CIR</i> | 715 | 1.070093 | 0.000128 | 0.009188 |
| <i>PARD6G-ASI</i> | 1E+08 | 1.217851 | 0.000131 | 0.009321 |
| <i>ACTA1</i> | 58 | 1.331674 | 0.000135 | 0.009519 |
| <i>GFAP</i> | 2670 | 1.269316 | 0.000145 | 0.010046 |
| <i>MYOD1</i> | 4654 | 2.388949 | 0.000145 | 0.010046 |
| <i>CRYAB</i> | 1410 | 1.14584 | 0.000146 | 0.010102 |
| <i>TGIF1</i> | 7050 | 1.19874 | 0.000147 | 0.010102 |
| <i>CASZ1</i> | 54897 | 1.483343 | 0.000147 | 0.010111 |
| <i>HSD3B7</i> | 80270 | 1.046229 | 0.000152 | 0.010377 |
| <i>PDE6G</i> | 5148 | 2.015065 | 0.000155 | 0.010437 |
| <i>PLAU</i> | 5328 | 1.5526 | 0.000154 | 0.010437 |
| <i>MC1R</i> | 4157 | 1.199393 | 0.000169 | 0.01091 |
| <i>TGFB3</i> | 7043 | 1.235542 | 0.000168 | 0.01091 |
| <i>PLEKHG4B</i> | 153478 | 1.746974 | 0.000175 | 0.010965 |
| <i>GADD45A</i> | 1647 | 1.027938 | 0.000172 | 0.010965 |
| <i>ITGA5</i> | 3678 | 1.1593 | 0.000174 | 0.010965 |
| <i>SRGN</i> | 5552 | 1.191171 | 0.00017 | 0.010965 |
| <i>RGS16</i> | 6004 | 1.330635 | 0.000172 | 0.010965 |
| <i>HASPIN</i> | 83903 | 1.969129 | 0.000172 | 0.010965 |
| <i>SIX5</i> | 147912 | 1.692135 | 0.000178 | 0.010992 |
| <i>ARHGEF16</i> | 27237 | 1.599003 | 0.000177 | 0.010992 |
| <i>IL4R</i> | 3566 | 1.189951 | 0.000179 | 0.011024 |
| <i>FIBCD1</i> | 84929 | 1.185489 | 0.000186 | 0.011291 |
| <i>LRRC3-DT</i> | 1.01E+08 | 1.843629 | 0.000189 | 0.011316 |
| <i>CENPM</i> | 79019 | 1.749863 | 0.000189 | 0.011316 |
| <i>ITGB2</i> | 3689 | 1.109521 | 0.000195 | 0.01144 |
| <i>IL21R</i> | 50615 | 1.817709 | 0.000195 | 0.01144 |
| <i>TRIM56</i> | 81844 | 1.236432 | 0.000199 | 0.011655 |
| <i>AOC1</i> | 26 | 2.11674 | 0.000206 | 0.011944 |
| <i>ZFP36</i> | 7538 | 1.968652 | 0.00021 | 0.012049 |

| | | | | |
|-------------------|----------|----------|----------|----------|
| <i>TMC8</i> | 147138 | 1.221872 | 0.000213 | 0.012146 |
| <i>JARID2-ASI</i> | 1.01E+08 | 1.537192 | 0.000219 | 0.012352 |
| <i>GDF15</i> | 9518 | 1.805335 | 0.00022 | 0.012352 |
| <i>MTRNR2L8</i> | 1E+08 | 2.367801 | 0.000237 | 0.012752 |
| <i>CDCP1</i> | 64866 | 1.395614 | 0.000237 | 0.012752 |
| <i>TGM2</i> | 7052 | 1.111706 | 0.000236 | 0.012752 |
| <i>FAM157A</i> | 728262 | 1.156561 | 0.000239 | 0.012752 |
| <i>ADAT3</i> | 113179 | 1.397216 | 0.000245 | 0.012866 |
| <i>TENT5A</i> | 55603 | 1.079824 | 0.000245 | 0.012866 |
| <i>UCP2</i> | 7351 | 1.285435 | 0.000245 | 0.012866 |
| <i>LINC01799</i> | 1.01E+08 | -3.42367 | 0.000264 | 0.013531 |
| <i>SERPINA1</i> | 5265 | 1.496322 | 0.000265 | 0.013531 |
| <i>PTGS2</i> | 5743 | 1.365405 | 0.000267 | 0.013559 |
| <i>SI00A9</i> | 6280 | 2.091003 | 0.000273 | 0.013757 |
| <i>FOXI3</i> | 344167 | 2.229069 | 0.000278 | 0.013874 |
| <i>RAB20</i> | 55647 | 1.151827 | 0.000279 | 0.013895 |
| <i>GBP3</i> | 2635 | 1.203617 | 0.000293 | 0.014354 |
| <i>TRIP10</i> | 9322 | 1.158444 | 0.000294 | 0.014394 |
| <i>ODF3B</i> | 440836 | 1.398597 | 0.0003 | 0.014635 |
| <i>APLNR</i> | 187 | 1.344786 | 0.000315 | 0.01496 |
| <i>TPRX1</i> | 284355 | 3.160382 | 0.000311 | 0.01496 |
| <i>SMTN</i> | 6525 | 1.000043 | 0.000315 | 0.01496 |
| <i>PIK3API</i> | 118788 | 1.033297 | 0.000318 | 0.014965 |
| <i>SPDYC</i> | 387778 | 2.001067 | 0.000317 | 0.014965 |
| <i>FAM167B</i> | 84734 | 1.690383 | 0.000316 | 0.014965 |
| <i>LRG1</i> | 116844 | 1.699128 | 0.000331 | 0.015039 |
| <i>TOR4A</i> | 54863 | 1.305638 | 0.000326 | 0.015039 |
| <i>ENGASE</i> | 64772 | 1.010838 | 0.000336 | 0.015039 |
| <i>TYROBP</i> | 7305 | 1.132782 | 0.000335 | 0.015039 |
| <i>IFITM1</i> | 8519 | 1.297772 | 0.000333 | 0.015039 |
| <i>TLR2</i> | 7097 | 1.131961 | 0.000359 | 0.01586 |
| <i>SSTR5-ASI</i> | 146336 | 2.476533 | 0.000367 | 0.016088 |

| | | | | |
|------------------|----------|----------|----------|----------|
| <i>SBNO2</i> | 22904 | 1.102491 | 0.000371 | 0.01621 |
| <i>CIQA</i> | 712 | 1.145656 | 0.000378 | 0.016392 |
| <i>TNC</i> | 3371 | 1.463355 | 0.00038 | 0.016433 |
| <i>PRSS42P</i> | 339906 | 2.330458 | 0.00039 | 0.016824 |
| <i>APOLD1</i> | 81575 | 1.090781 | 0.000412 | 0.017479 |
| <i>MIR3976HG</i> | 645355 | -1.59725 | 0.000424 | 0.017807 |
| <i>F2RL3</i> | 9002 | 1.766242 | 0.000426 | 0.017863 |
| <i>COL4A1</i> | 1282 | 1.110451 | 0.00045 | 0.018551 |
| <i>MTIL</i> | 4500 | 1.440857 | 0.000454 | 0.018655 |
| <i>ADAMTS1</i> | 9510 | 1.009682 | 0.000455 | 0.018664 |
| <i>TNFSF9</i> | 8744 | 1.185339 | 0.000458 | 0.018698 |
| <i>EMP3</i> | 2014 | 1.192011 | 0.000476 | 0.01915 |
| <i>NLRC5</i> | 84166 | 1.360701 | 0.000479 | 0.019155 |
| <i>PPP1R13L</i> | 10848 | 1.136402 | 0.000482 | 0.019165 |
| <i>NR4A1</i> | 3164 | 1.359261 | 0.000496 | 0.019629 |
| <i>FOXJ1</i> | 2302 | 1.695987 | 0.000502 | 0.019643 |
| <i>TCF15</i> | 6939 | 1.332408 | 0.000522 | 0.020173 |
| <i>PLSCR3</i> | 57048 | 1.998938 | 0.000525 | 0.020214 |
| <i>ND3</i> | 4537 | 1.404757 | 0.000529 | 0.020284 |
| <i>IFI44L</i> | 10964 | 1.28398 | 0.000539 | 0.020515 |
| <i>CLDN6</i> | 9074 | 1.65119 | 0.000538 | 0.020515 |
| <i>TDRD10</i> | 126668 | 1.347944 | 0.000556 | 0.021024 |
| <i>KIF1C</i> | 10749 | 1.106094 | 0.000566 | 0.021134 |
| <i>PNP</i> | 4860 | 1.041275 | 0.000597 | 0.021885 |
| <i>TEKT4</i> | 150483 | 2.04352 | 0.00061 | 0.022212 |
| <i>HBB</i> | 3043 | 1.609588 | 0.000612 | 0.02224 |
| <i>MVP</i> | 9961 | 1.083501 | 0.000661 | 0.023434 |
| <i>MMEL1</i> | 79258 | 1.994029 | 0.000674 | 0.023675 |
| <i>MIR4516</i> | 1.01E+08 | 1.467787 | 0.000684 | 0.023921 |
| <i>TSSK6</i> | 83983 | 1.043211 | 0.000714 | 0.024396 |
| <i>SAMD11</i> | 148398 | 1.734106 | 0.000727 | 0.024665 |
| <i>HBM</i> | 3042 | 2.166348 | 0.000748 | 0.02514 |

| | | | | |
|--------------------|----------|----------|----------|----------|
| <i>LHB</i> | 3972 | 1.630834 | 0.000748 | 0.02514 |
| <i>CD300A</i> | 11314 | 1.074829 | 0.000764 | 0.025304 |
| <i>SOCS1</i> | 8651 | 1.788552 | 0.000763 | 0.025304 |
| <i>TRARG1</i> | 286753 | 1.529783 | 0.000766 | 0.025322 |
| <i>PLP2</i> | 5355 | 1.291133 | 0.000779 | 0.025424 |
| <i>PLEKHA4</i> | 57664 | 1.415673 | 0.00078 | 0.025424 |
| <i>LAPTM5</i> | 7805 | 1.071379 | 0.000779 | 0.025424 |
| <i>DNASE1L2</i> | 1775 | 1.141355 | 0.000784 | 0.025527 |
| <i>WWTR1</i> | 25937 | 1.015353 | 0.000805 | 0.025978 |
| <i>TREM2</i> | 54209 | 1.120219 | 0.000805 | 0.025978 |
| <i>TM4SF1-ASI</i> | 1.01E+08 | -3.36441 | 0.000826 | 0.026484 |
| <i>IRX1</i> | 79192 | 2.5444 | 0.00083 | 0.026522 |
| <i>CYP21A1P</i> | 1590 | 1.611097 | 0.000836 | 0.026604 |
| <i>VSIG4</i> | 11326 | 1.376054 | 0.00088 | 0.027684 |
| <i>FCER1G</i> | 2207 | 1.526436 | 0.000882 | 0.02771 |
| <i>LINC02192</i> | 1.01E+08 | -1.13801 | 0.000903 | 0.028129 |
| <i>ITPRIP</i> | 85450 | 1.060705 | 0.0009 | 0.028129 |
| <i>CPAMD8</i> | 27151 | 1.09147 | 0.000913 | 0.028214 |
| <i>TM4SF1</i> | 4071 | 1.095555 | 0.00093 | 0.028487 |
| <i>LDLRAD2</i> | 401944 | 1.951368 | 0.000932 | 0.028495 |
| <i>ENTPD8</i> | 377841 | 1.493886 | 0.000938 | 0.028614 |
| <i>GCNT3</i> | 9245 | 1.607383 | 0.000974 | 0.029277 |
| <i>CP</i> | 1356 | 1.565941 | 0.000998 | 0.029651 |
| <i>FGF18</i> | 8817 | 1.164056 | 0.001002 | 0.029714 |
| <i>GDF5</i> | 8200 | 1.731794 | 0.001015 | 0.029971 |
| <i>SLC6A12-ASI</i> | 1.02E+08 | 1.703735 | 0.001034 | 0.030408 |
| <i>LINC01588</i> | 283551 | 1.341779 | 0.001077 | 0.031052 |
| <i>CLEC18B</i> | 497190 | 1.545066 | 0.001107 | 0.031615 |
| <i>LINC01224</i> | 1.04E+08 | 1.452484 | 0.001114 | 0.03164 |
| <i>PRSS40A</i> | 150527 | 2.85804 | 0.001117 | 0.03164 |
| <i>CAPS</i> | 828 | 1.058605 | 0.001116 | 0.03164 |
| <i>LINC01354</i> | 1.01E+08 | 1.038977 | 0.00115 | 0.031955 |

| | | | | |
|------------------|----------|----------|----------|----------|
| <i>TLL10</i> | 254173 | 2.480889 | 0.001143 | 0.031955 |
| <i>ANGPTL4</i> | 51129 | 1.169107 | 0.00114 | 0.031955 |
| <i>LINC01143</i> | 1.04E+08 | 3.10912 | 0.001164 | 0.032167 |
| <i>SCARNA17</i> | 677769 | 1.057557 | 0.001161 | 0.032167 |
| <i>MSLN</i> | 10232 | 1.51505 | 0.001181 | 0.032383 |
| <i>MIR661</i> | 724031 | 1.828246 | 0.001188 | 0.032423 |
| <i>NOS3</i> | 4846 | 1.068102 | 0.001241 | 0.03344 |
| <i>SMPX</i> | 23676 | -1.1548 | 0.001277 | 0.033967 |
| <i>CABP4</i> | 57010 | 1.229218 | 0.001284 | 0.034115 |
| <i>SELE</i> | 6401 | 1.872371 | 0.001304 | 0.034418 |
| <i>CCDC33</i> | 80125 | 1.744076 | 0.001429 | 0.036437 |
| <i>LINC01554</i> | 202299 | 1.383167 | 0.001457 | 0.036918 |
| <i>DNMT3L</i> | 29947 | 1.792066 | 0.001491 | 0.037477 |
| <i>CYP27C1</i> | 339761 | 1.3919 | 0.001491 | 0.037477 |
| <i>GPR4</i> | 2828 | 1.391017 | 0.0015 | 0.037576 |
| <i>CLDN19</i> | 149461 | 1.951732 | 0.001525 | 0.037823 |
| <i>MLKL</i> | 197259 | 1.264725 | 0.001524 | 0.037823 |
| <i>IL4I1</i> | 259307 | 1.582605 | 0.001538 | 0.037823 |
| <i>C9orf50</i> | 375759 | 1.008132 | 0.001523 | 0.037823 |
| <i>CT66</i> | 1.01E+08 | 1.750894 | 0.001564 | 0.03814 |
| <i>ELF4</i> | 2000 | 1.0827 | 0.001568 | 0.03814 |
| <i>GNG8</i> | 94235 | 1.659157 | 0.001567 | 0.03814 |
| <i>UPB1</i> | 51733 | 1.192704 | 0.001617 | 0.038904 |
| <i>TEX11</i> | 56159 | 1.782515 | 0.001637 | 0.039086 |
| <i>PDPN</i> | 10630 | 1.102655 | 0.001689 | 0.039798 |
| <i>KIAA0040</i> | 9674 | 1.011151 | 0.001701 | 0.039869 |
| <i>CNN2</i> | 1265 | 1.069162 | 0.001711 | 0.039905 |
| <i>C5orf60</i> | 285679 | 1.830569 | 0.001716 | 0.039969 |
| <i>CH25H</i> | 9023 | 1.238515 | 0.001739 | 0.040205 |
| <i>PSG5</i> | 5673 | -1.14458 | 0.001747 | 0.040267 |
| <i>AATBC</i> | 284837 | 1.056306 | 0.001757 | 0.040392 |
| <i>MAMDC4</i> | 158056 | 1.110201 | 0.001806 | 0.041033 |

| | | | | |
|------------------|--------|----------|----------|----------|
| <i>GRK1</i> | 6011 | 1.124643 | 0.001812 | 0.041042 |
| <i>SLCIA7</i> | 6512 | 1.331661 | 0.001836 | 0.041354 |
| <i>OR2B11</i> | 127623 | 1.732429 | 0.001846 | 0.041407 |
| <i>TMPRSS13</i> | 84000 | 1.544543 | 0.001888 | 0.042173 |
| <i>MBOAT4</i> | 619373 | 1.351221 | 0.001931 | 0.042426 |
| <i>RNF122</i> | 79845 | 1.116363 | 0.00193 | 0.042426 |
| <i>C14orf178</i> | 283579 | 1.504854 | 0.001959 | 0.04289 |
| <i>LCN8</i> | 138307 | 1.359008 | 0.001977 | 0.043132 |
| <i>MFSD6L</i> | 162387 | 2.1021 | 0.001993 | 0.043312 |
| <i>EMPI1</i> | 2012 | 1.691395 | 0.002006 | 0.043411 |
| <i>OTOP3</i> | 347741 | 2.263111 | 0.00202 | 0.043444 |
| <i>SELENOV</i> | 348303 | 1.615439 | 0.002078 | 0.044289 |
| <i>GZMM</i> | 3004 | 1.535053 | 0.002089 | 0.044415 |
| <i>FCGR3A</i> | 2214 | 1.036038 | 0.0021 | 0.044453 |
| <i>MIR149</i> | 406941 | 1.539452 | 0.002125 | 0.044531 |
| <i>MROH6</i> | 642475 | 1.127593 | 0.002119 | 0.044531 |
| <i>SERPINE1</i> | 5054 | 1.669014 | 0.002149 | 0.044935 |
| <i>TSPAN16</i> | 26526 | 1.186533 | 0.002157 | 0.044938 |
| <i>LRRC71</i> | 149499 | 1.354011 | 0.002162 | 0.044987 |
| <i>CILP2</i> | 148113 | 1.249929 | 0.002249 | 0.046071 |
| <i>LINC02418</i> | 1E+08 | -1.21436 | 0.002272 | 0.046248 |
| <i>MMP25</i> | 64386 | 1.314055 | 0.002439 | 0.048635 |
| <i>RNA5SI3</i> | 1E+08 | 3.025204 | 0.002481 | 0.049195 |
| <i>ASCL2</i> | 430 | 1.395338 | 0.002487 | 0.049204 |
| <i>BATF2</i> | 116071 | 1.198966 | 0.002527 | 0.049539 |
| <i>PAX2</i> | 5076 | 1.265916 | 0.00254 | 0.049702 |
| <i>SEMG2</i> | 6407 | -2.41159 | 0.002564 | 0.049967 |
| <i>PRIMA1</i> | 145270 | 1.170896 | 0.002598 | 0.050196 |
| <i>HIPK2</i> | 28996 | 1.070251 | 0.002631 | 0.050427 |
| <i>ITGB4</i> | 3691 | 1.029559 | 0.002652 | 0.050777 |
| <i>CXCL3</i> | 2921 | 1.828203 | 0.002672 | 0.05107 |
| <i>MTRNR2L1</i> | 1E+08 | 2.632282 | 0.002687 | 0.051203 |

| | | | | |
|--------------------|----------|----------|----------|----------|
| <i>HMI3-ASI</i> | 1.01E+08 | 1.480581 | 0.002719 | 0.051394 |
| <i>IL1B</i> | 3553 | 1.471316 | 0.002726 | 0.051484 |
| <i>RAPSN</i> | 5913 | 1.932399 | 0.002734 | 0.051489 |
| <i>NFE2</i> | 4778 | 1.614367 | 0.002746 | 0.051622 |
| <i>PRICKLE3</i> | 4007 | 1.047567 | 0.002757 | 0.051643 |
| <i>SPINT1</i> | 6692 | 1.157864 | 0.002755 | 0.051643 |
| <i>GUCA1C</i> | 9626 | -1.58509 | 0.00278 | 0.051925 |
| <i>CARD9</i> | 64170 | 1.095892 | 0.002802 | 0.052076 |
| <i>LINC00924</i> | 145820 | -1.2958 | 0.002811 | 0.052079 |
| <i>SYNPR-ASI</i> | 1.01E+08 | -1.30538 | 0.002855 | 0.052508 |
| <i>CFAP45</i> | 25790 | 1.413027 | 0.002857 | 0.052508 |
| <i>TCIRG1</i> | 10312 | 1.009494 | 0.002915 | 0.05324 |
| <i>RAB43</i> | 339122 | 1.08007 | 0.002919 | 0.05328 |
| <i>RBM47</i> | 54502 | 1.027081 | 0.002994 | 0.054066 |
| <i>CPT1B</i> | 1375 | 1.297586 | 0.003008 | 0.054267 |
| <i>TNNC1</i> | 7134 | 1.50506 | 0.003155 | 0.056187 |
| <i>OR5B12</i> | 390191 | -2.41363 | 0.003173 | 0.056457 |
| <i>SNORD114-17</i> | 767595 | -1.12127 | 0.003202 | 0.05685 |
| <i>KRT40</i> | 125115 | -1.92244 | 0.003285 | 0.057447 |
| <i>CXCLI</i> | 2919 | 1.858962 | 0.003282 | 0.057447 |
| <i>LINC02709</i> | 440028 | 1.088645 | 0.003274 | 0.057447 |
| <i>BCL3</i> | 602 | 1.153026 | 0.003317 | 0.057916 |
| <i>CABP2</i> | 51475 | 2.83977 | 0.003371 | 0.058376 |
| <i>LAIR1</i> | 3903 | 1.292494 | 0.003405 | 0.058813 |
| <i>MMP11</i> | 4320 | 1.239467 | 0.003474 | 0.059609 |
| <i>VTRNA1-3</i> | 56662 | 1.684531 | 0.003488 | 0.05969 |
| <i>HOXB7</i> | 3217 | 2.370539 | 0.003505 | 0.059933 |
| <i>SPATA12</i> | 353324 | 1.443686 | 0.00351 | 0.059933 |
| <i>EGR4</i> | 1961 | 1.037684 | 0.00352 | 0.059997 |
| <i>SPINK6</i> | 404203 | -1.2844 | 0.003533 | 0.060075 |
| <i>CERKL</i> | 375298 | -1.0625 | 0.003613 | 0.060783 |
| <i>CFAP73</i> | 387885 | 1.158718 | 0.00362 | 0.06085 |

| | | | | |
|---------------------|----------|----------|----------|----------|
| <i>H19</i> | 283120 | 1.052814 | 0.003631 | 0.060983 |
| <i>APOC1</i> | 341 | 1.06314 | 0.003647 | 0.061107 |
| <i>PKDIP6</i> | 353511 | 1.035885 | 0.003646 | 0.061107 |
| <i>TK1</i> | 7083 | 1.062786 | 0.003674 | 0.061363 |
| <i>HCST</i> | 10870 | 1.058886 | 0.003705 | 0.061528 |
| <i>AKAIN1</i> | 642597 | -1.02583 | 0.00374 | 0.061846 |
| <i>OVOL3</i> | 728361 | 1.224566 | 0.003762 | 0.061917 |
| <i>WWC2-AS2</i> | 152641 | 1.304611 | 0.003791 | 0.062206 |
| <i>C2CD4A</i> | 145741 | 1.067767 | 0.00382 | 0.062387 |
| <i>AQP5</i> | 362 | 1.169627 | 0.003862 | 0.06267 |
| <i>USP17L19</i> | 1E+08 | 1.615847 | 0.003887 | 0.06302 |
| <i>NAT16</i> | 375607 | 1.069305 | 0.003895 | 0.063111 |
| <i>PPP1R18</i> | 170954 | 1.143954 | 0.003911 | 0.063232 |
| <i>TIMP1</i> | 7076 | 1.067739 | 0.003929 | 0.063336 |
| <i>CTRB2</i> | 440387 | 1.905965 | 0.003938 | 0.06336 |
| <i>CFAP99</i> | 402160 | 1.218486 | 0.004021 | 0.064234 |
| <i>CTF1</i> | 1489 | 1.08676 | 0.004044 | 0.064368 |
| <i>FOXP4-AS1</i> | 1.01E+08 | 1.57093 | 0.004083 | 0.064772 |
| <i>LINC01876</i> | 1.02E+08 | -1.74019 | 0.004097 | 0.064894 |
| <i>LINC01478</i> | 1.02E+08 | -1.34512 | 0.004108 | 0.065018 |
| <i>SLC12A3</i> | 6559 | 1.539515 | 0.004121 | 0.065143 |
| <i>PIRT</i> | 644139 | 1.283811 | 0.004137 | 0.065281 |
| <i>NTN3</i> | 4917 | 1.006471 | 0.00416 | 0.065502 |
| <i>TNFRSF8</i> | 943 | 1.878377 | 0.004183 | 0.065708 |
| <i>LOC101927727</i> | 1.02E+08 | 1.164057 | 0.00422 | 0.066082 |
| <i>LRRC18</i> | 474354 | 1.274474 | 0.004359 | 0.067441 |
| <i>OAS2</i> | 4939 | 1.062914 | 0.004401 | 0.067616 |
| <i>OR13C4</i> | 138804 | -1.97392 | 0.004456 | 0.068174 |
| <i>SIGLEC1</i> | 6614 | 1.307587 | 0.004459 | 0.068174 |
| <i>LINC00528</i> | 200298 | 1.501346 | 0.004534 | 0.068892 |
| <i>GDNF</i> | 2668 | 1.347511 | 0.004547 | 0.068952 |
| <i>KCNQ1</i> | 3784 | 1.033129 | 0.00471 | 0.070393 |

| | | | | |
|-------------------|--------|----------|----------|----------|
| <i>DYNLT4</i> | 343521 | 1.545828 | 0.00477 | 0.071041 |
| <i>DPY19L3-DT</i> | 400684 | 1.265545 | 0.004796 | 0.071264 |
| <i>C19orf67</i> | 646457 | 1.144443 | 0.004789 | 0.071264 |
| <i>ZAP70</i> | 7535 | 1.137074 | 0.004808 | 0.071396 |
| <i>SLC23A3</i> | 151295 | 1.310699 | 0.004818 | 0.071441 |
| <i>PRAMI</i> | 84106 | 1.092004 | 0.004835 | 0.071615 |
| <i>CATSPER1</i> | 117144 | 1.669311 | 0.004862 | 0.07188 |
| <i>MTRNR2L2</i> | 1E+08 | 2.44574 | 0.004954 | 0.072387 |
| <i>C2CD4B</i> | 388125 | 1.580573 | 0.004963 | 0.072387 |
| <i>OR2G6</i> | 391211 | -1.74366 | 0.004964 | 0.072387 |
| <i>LRRC25</i> | 126364 | 1.090599 | 0.005128 | 0.073654 |
| <i>SMIM1</i> | 388588 | 1.399279 | 0.005135 | 0.073702 |
| <i>HAMP</i> | 57817 | 1.226888 | 0.005242 | 0.074519 |
| <i>DPEP3</i> | 64180 | 1.227312 | 0.005348 | 0.075292 |
| <i>DPT</i> | 1805 | -1.00655 | 0.005405 | 0.075737 |
| <i>IRGM</i> | 345611 | 1.313883 | 0.005398 | 0.075737 |
| <i>GCOM1</i> | 145781 | -1.4212 | 0.005439 | 0.075927 |
| <i>DUOXA1</i> | 90527 | 1.318874 | 0.00544 | 0.075927 |
| <i>SULT1C2P1</i> | 151234 | -1.35423 | 0.005482 | 0.076195 |
| <i>STC1</i> | 6781 | 1.324434 | 0.005513 | 0.076376 |
| <i>PLA2G4E</i> | 123745 | 1.390556 | 0.005522 | 0.076449 |
| <i>SAG</i> | 6295 | 1.396071 | 0.005534 | 0.076461 |
| <i>OVOLI</i> | 5017 | 1.451633 | 0.005587 | 0.076836 |
| <i>LINC02875</i> | 388407 | 1.598003 | 0.005661 | 0.07743 |
| <i>CRTAM</i> | 56253 | -1.13991 | 0.005678 | 0.077524 |
| <i>UBE2C</i> | 11065 | 1.535035 | 0.005739 | 0.077683 |
| <i>FFAR2</i> | 2867 | 2.028285 | 0.005731 | 0.077683 |
| <i>LRRC26</i> | 389816 | 1.832309 | 0.005739 | 0.077683 |
| <i>FOXF1</i> | 2294 | 1.292522 | 0.005759 | 0.077847 |
| <i>COX2</i> | 4513 | 1.237483 | 0.005776 | 0.077927 |
| <i>ADGRE1</i> | 2015 | 1.577064 | 0.00584 | 0.078109 |
| <i>SH2D6</i> | 284948 | 1.095818 | 0.005838 | 0.078109 |

| | | | | |
|--------------------|----------|----------|----------|----------|
| <i>ANXA2</i> | 302 | 1.087795 | 0.005828 | 0.078109 |
| <i>MYO18B</i> | 84700 | 1.017854 | 0.005802 | 0.078109 |
| <i>KRTAP5-1</i> | 387264 | 1.39696 | 0.005894 | 0.078543 |
| <i>TLR9</i> | 54106 | 1.686645 | 0.005894 | 0.078543 |
| <i>SERPINA4</i> | 5267 | 2.075329 | 0.005999 | 0.079414 |
| <i>TNFRSF10D</i> | 8793 | 1.040265 | 0.006218 | 0.081065 |
| <i>PLAC8</i> | 51316 | 1.189626 | 0.00623 | 0.081129 |
| <i>CEBPE</i> | 1053 | 2.050308 | 0.006304 | 0.081698 |
| <i>LINC00347</i> | 338864 | -1.50337 | 0.006353 | 0.082158 |
| <i>CLRN3</i> | 119467 | -1.43141 | 0.006462 | 0.082954 |
| <i>CAI2</i> | 771 | 1.136338 | 0.006458 | 0.082954 |
| <i>CACTIN-ASI</i> | 404665 | 1.436747 | 0.0065 | 0.083281 |
| <i>C5orf64-ASI</i> | 1.01E+08 | 1.181087 | 0.006509 | 0.083295 |
| <i>TPIIP2</i> | 286016 | 1.003028 | 0.006508 | 0.083295 |
| <i>TNFSF14</i> | 8740 | 1.414925 | 0.006554 | 0.083404 |
| <i>TLCD2</i> | 727910 | 1.085945 | 0.006634 | 0.08406 |
| <i>LBX2</i> | 85474 | 1.579046 | 0.006735 | 0.084976 |
| <i>FXVD3</i> | 5349 | 1.014006 | 0.006767 | 0.08522 |
| <i>MAFA</i> | 389692 | 1.831581 | 0.006806 | 0.085554 |
| <i>PAQR6</i> | 79957 | 1.028522 | 0.006836 | 0.085781 |
| <i>ADORA2A</i> | 135 | 1.585538 | 0.006852 | 0.085813 |
| <i>SPOCD1</i> | 90853 | 1.695552 | 0.006856 | 0.085813 |
| <i>TMEM210</i> | 1.01E+08 | 1.600959 | 0.006958 | 0.086493 |
| <i>BCAR4</i> | 400500 | 1.629018 | 0.00698 | 0.08654 |
| <i>OR52E6</i> | 390078 | -2.35868 | 0.006992 | 0.08658 |
| <i>LMO7DN</i> | 729420 | -1.33128 | 0.007033 | 0.086672 |
| <i>ZNRF4</i> | 148066 | 1.656437 | 0.007052 | 0.086769 |
| <i>WNT3A</i> | 89780 | 1.894303 | 0.007104 | 0.087022 |
| <i>LINC01793</i> | 1.02E+08 | -1.08822 | 0.007134 | 0.087189 |
| <i>PCDHB1</i> | 29930 | 1.15345 | 0.007183 | 0.087624 |
| <i>MUC2</i> | 4583 | 1.58002 | 0.007325 | 0.088464 |
| <i>DOK7</i> | 285489 | 1.006896 | 0.007334 | 0.088481 |

| | | | | |
|---------------------|----------|----------|----------|----------|
| <i>LOC102724421</i> | 1.03E+08 | -1.6757 | 0.007375 | 0.08866 |
| <i>C11orf91</i> | 1E+08 | 1.505707 | 0.007409 | 0.08896 |
| <i>HCAR3</i> | 8843 | 1.692873 | 0.007479 | 0.089492 |
| <i>GTSE1</i> | 51512 | 1.497741 | 0.00751 | 0.089705 |
| <i>TEAD4</i> | 7004 | 1.292904 | 0.007525 | 0.089779 |
| <i>SSMEM1</i> | 136263 | -2.2774 | 0.007541 | 0.089926 |
| <i>LINC01426</i> | 1.01E+08 | 1.434712 | 0.007606 | 0.090357 |
| <i>LOC105371899</i> | 1.05E+08 | 1.118145 | 0.007645 | 0.090357 |
| <i>TEPP</i> | 374739 | 1.253275 | 0.007651 | 0.090357 |
| <i>SLC22A11</i> | 55867 | 1.749717 | 0.007593 | 0.090357 |
| <i>OPTC</i> | 26254 | 1.242466 | 0.007805 | 0.091597 |
| <i>HI-5</i> | 3009 | 1.607219 | 0.007967 | 0.09239 |
| <i>IRF9</i> | 10379 | 1.15315 | 0.008063 | 0.093039 |
| <i>PBK</i> | 55872 | 1.650466 | 0.008066 | 0.093039 |
| <i>TLX1</i> | 3195 | -2.48117 | 0.008113 | 0.093089 |
| <i>DPRXP4</i> | 503645 | 1.389419 | 0.008114 | 0.093089 |
| <i>IL22RA1</i> | 58985 | 1.843308 | 0.008254 | 0.093693 |
| <i>MIR3680-1</i> | 1.01E+08 | 1.041817 | 0.008319 | 0.094195 |
| <i>CCL2</i> | 6347 | 1.782402 | 0.00835 | 0.094488 |
| <i>LINC01659</i> | 1.02E+08 | 1.291491 | 0.008564 | 0.095598 |
| <i>RNA5S11</i> | 1E+08 | 3.443435 | 0.008598 | 0.095621 |
| <i>LILRB3</i> | 11025 | 1.268371 | 0.008577 | 0.095621 |
| <i>MS4A12</i> | 54860 | -2.2667 | 0.008711 | 0.09605 |
| <i>OSM</i> | 5008 | 1.488639 | 0.008739 | 0.096258 |
| <i>SIGLEC12</i> | 89858 | 1.737658 | 0.008815 | 0.096816 |
| <i>GALNT4</i> | 8693 | 1.364773 | 0.008896 | 0.097361 |
| <i>PRG4</i> | 10216 | -1.03291 | 0.00896 | 0.097936 |
| <i>CD1D</i> | 912 | 1.159017 | 0.008963 | 0.097936 |
| <i>LINC02728</i> | 1.02E+08 | -1.26149 | 0.008991 | 0.098047 |
| <i>MISP</i> | 126353 | 1.280916 | 0.00904 | 0.098309 |
| <i>GALNT5</i> | 11227 | -1.32272 | 0.009085 | 0.098515 |
| <i>CTRC</i> | 11330 | 1.223551 | 0.009097 | 0.098515 |

| | | | | |
|--------------------|----------|----------|----------|----------|
| <i>AGTR2</i> | 186 | -1.8679 | 0.009214 | 0.099259 |
| <i>LINC01922</i> | 1.02E+08 | 2.183066 | 0.009235 | 0.099308 |
| <i>GDPD4</i> | 220032 | 1.272959 | 0.009238 | 0.099308 |
| <i>LINC01618</i> | 152578 | -1.7553 | 0.009294 | 0.09981 |
| <i>RAB42</i> | 115273 | 1.119902 | 0.009344 | 0.100142 |
| <i>REG3G</i> | 130120 | -2.32413 | 0.009343 | 0.100142 |
| <i>FOXL1</i> | 2300 | 1.06727 | 0.009415 | 0.100581 |
| <i>CXCL8</i> | 3576 | 1.322078 | 0.009509 | 0.101268 |
| <i>ADGRF4</i> | 221393 | -1.38129 | 0.009643 | 0.102123 |
| <i>FSCN3</i> | 29999 | 1.592507 | 0.009849 | 0.102985 |
| <i>CYP19A1</i> | 1588 | 1.450437 | 0.009887 | 0.103068 |
| <i>CLDN7</i> | 1366 | 1.047682 | 0.009902 | 0.103073 |
| <i>LINC00163</i> | 727699 | 1.651412 | 0.009956 | 0.103466 |
| <i>SNORD115-39</i> | 1E+08 | 1.086384 | 0.009711 | NA |
| <i>RBPM5-AS1</i> | 1E+08 | 1.759077 | 0.009141 | NA |
| <i>MIR1915</i> | 1E+08 | 2.286234 | 0.001604 | NA |
| <i>MIR4316</i> | 1E+08 | 2.574339 | 0.005938 | NA |
| <i>MIR3181</i> | 1E+08 | 1.951211 | 0.009556 | NA |
| <i>MIR3197</i> | 1E+08 | 3.689881 | 7.49E-05 | NA |
| <i>MIR3909</i> | 1.01E+08 | 1.949571 | 0.002912 | NA |
| <i>LINC01718</i> | 1.01E+08 | 3.61376 | 0.00472 | NA |
| <i>MIR4466</i> | 1.01E+08 | 2.039839 | 0.009263 | NA |
| <i>MIR4449</i> | 1.01E+08 | 2.121267 | 0.003325 | NA |
| <i>MIR4479</i> | 1.01E+08 | 1.814136 | 0.007267 | NA |
| <i>LINC00492</i> | 1.01E+08 | -3.33268 | 0.002103 | NA |
| <i>ZFX-AS1</i> | 1.01E+08 | 1.376862 | 0.008966 | NA |
| <i>LINC00358</i> | 1.01E+08 | -3.74364 | 0.000421 | NA |
| <i>COL4A2-AS1</i> | 1.01E+08 | 2.058727 | 0.001099 | NA |
| <i>LINC01216</i> | 1.01E+08 | -3.10369 | 0.000991 | NA |
| <i>LINC02402</i> | 1.02E+08 | 3.170078 | 0.004008 | NA |
| <i>LINC01708</i> | 1.02E+08 | -3.23468 | 0.008736 | NA |
| <i>PLA2G4E-AS1</i> | 1.02E+08 | 1.821313 | 0.002986 | NA |

| | | | | |
|---------------------|----------|----------|----------|----|
| <i>LOC101929536</i> | 1.02E+08 | 1.796051 | 0.001065 | NA |
| <i>LINC01058</i> | 1.04E+08 | 2.10803 | 0.000885 | NA |
| <i>CELP</i> | 1057 | 2.293706 | 0.00211 | NA |
| <i>OR5I1</i> | 10798 | -3.58564 | 0.001286 | NA |
| <i>CGB2</i> | 114336 | 2.410039 | 0.009757 | NA |
| <i>OR6N1</i> | 128372 | 2.639826 | 0.005067 | NA |
| <i>SCP2D1</i> | 140856 | -3.19232 | 0.004576 | NA |
| <i>TRAV8-1</i> | 28685 | -2.52074 | 0.009049 | NA |
| <i>TRAV1-1</i> | 28693 | -4.09129 | 0.005246 | NA |
| <i>IGKV6D-21</i> | 28870 | -3.46924 | 0.00774 | NA |
| <i>HOXA9</i> | 3205 | 4.681392 | 0.002067 | NA |
| <i>KCNQ1-AS1</i> | 338653 | 3.097168 | 4.62E-05 | NA |
| <i>OR52L1</i> | 338751 | -1.96947 | 0.005797 | NA |
| <i>SYCN</i> | 342898 | 2.697877 | 0.003001 | NA |
| <i>LILRA5</i> | 353514 | 2.726068 | 0.000817 | NA |
| <i>OR52A5</i> | 390054 | -2.37944 | 0.007009 | NA |
| <i>OR6M1</i> | 390261 | -2.42269 | 0.004549 | NA |
| <i>OR7G2</i> | 390882 | -2.98857 | 0.004272 | NA |
| <i>CIBARIP2</i> | 403315 | 2.01028 | 0.008492 | NA |
| <i>MIR132</i> | 406921 | 2.827598 | 0.000195 | NA |
| <i>MIR212</i> | 406994 | 2.075189 | 0.001237 | NA |
| <i>RNASE13</i> | 440163 | 2.861922 | 0.000607 | NA |
| <i>CYMP-AS1</i> | 440602 | 1.969082 | 0.00967 | NA |
| <i>ATOH1</i> | 474 | 2.7333 | 0.005595 | NA |
| <i>PPDPFL</i> | 492307 | 1.786662 | 0.005376 | NA |
| <i>PRLH</i> | 51052 | 3.645554 | 0.000853 | NA |
| <i>DUSP21</i> | 63904 | 2.888804 | 0.003727 | NA |
| <i>FABP9</i> | 646480 | -2.70819 | 0.002269 | NA |
| <i>SPRR2F</i> | 6705 | 3.128219 | 0.007173 | NA |
| <i>SNORD62B</i> | 692093 | 1.44991 | 0.004328 | NA |
| <i>MIR602</i> | 693187 | 2.39804 | 0.009844 | NA |
| <i>ARL14</i> | 80117 | 2.420292 | 0.00384 | NA |

| | | | | |
|-----------------|-------|----------|----------|----|
| <i>MPIG6B</i> | 80739 | 1.534788 | 0.007776 | NA |
| <i>OR2B2</i> | 81697 | -2.47542 | 0.002937 | NA |
| <i>MIA</i> | 8190 | 2.152159 | 0.001749 | NA |
| <i>H3-4</i> | 8290 | 1.690598 | 0.007093 | NA |
| <i>C15orf48</i> | 84419 | 2.26261 | 0.006564 | NA |
| <i>GPR174</i> | 84636 | -2.29749 | 0.004062 | NA |
| <i>MBD3L1</i> | 85509 | 2.299661 | 0.006439 | NA |
| <i>UCN2</i> | 90226 | 2.405504 | 0.00181 | NA |
| <i>FTMT</i> | 94033 | 3.277739 | 0.003322 | NA |

Table 8.2. The differential expression genes DEGs of blood dataset (P -value < 0.01 , $-1 > \text{Log}_2\text{FC} > +1$), * Novel genes, NA no symbol ID

| Symbol | Ensembl ID | log2FoldChange | P-value | P-adj |
|-------------------|-----------------|----------------|-------------|-------------|
| <i>CXCL1</i> | ENSG00000163739 | 2.611602717 | 0.00000742 | 0.089229768 |
| <i>TNFAIP6</i> | ENSG00000123610 | 1.799753071 | 0.089229768 | |
| <i>TRIB3*</i> | ENSG00000101255 | -2.726146762 | 0.0000188 | 0.121223383 |
| <i>GCH1</i> | ENSG00000131979 | 1.198998008 | 0.0000374 | 0.181947932 |
| <i>CCL2</i> | ENSG00000108691 | 1.675389985 | 0.0000423 | 0.181947932 |
| <i>CCL23</i> | ENSG00000274736 | 1.96012341 | 0.000183082 | 0.393657267 |
| <i>SYNPO2*</i> | ENSG00000172403 | 3.50336981 | 0.000257933 | 0.439093898 |
| <i>IL1A</i> | ENSG00000115008 | 2.486405818 | 0.000300338 | 0.439093898 |
| <i>SLC39A8</i> | ENSG00000138821 | 1.368699557 | 0.000376551 | 0.462655263 |
| <i>CXCL10</i> | ENSG00000169245 | 1.968878262 | 0.000628524 | 0.50734157 |
| <i>CCL3</i> | ENSG00000277632 | 1.061085072 | 0.000772934 | 0.539006273 |
| <i>WWC2-AS2*</i> | ENSG00000251359 | 2.961915035 | 0.000817072 | 0.552064475 |
| <i>UPB1</i> | ENSG00000100024 | 2.728739755 | 0.00092418 | 0.593987671 |
| NA | ENSG00000276758 | 3.253834459 | 0.001287987 | 0.65061141 |
| <i>ETV5</i> | ENSG00000244405 | 1.321385714 | 0.001349342 | 0.65061141 |
| <i>TTC30A</i> | ENSG00000197557 | 1.428187366 | 0.00146891 | 0.65061141 |
| NA | ENSG00000210174 | -1.291393539 | 0.0014902 | 0.65061141 |
| <i>RN7SL239P*</i> | ENSG00000242999 | -3.141583004 | 0.001573124 | 0.65061141 |

| | | | | |
|------------------|-----------------|--------------|-------------|-------------|
| <i>RPL10P9</i> | ENSG00000233913 | 1.910385627 | 0.001864703 | 0.673109563 |
| <i>SERPINB2</i> | ENSG00000197632 | 1.254455656 | 0.002032955 | 0.673109563 |
| <i>PLEKHA8P1</i> | ENSG00000134297 | -1.489533346 | 0.002084396 | 0.674070977 |
| <i>SYT17</i> | ENSG00000103528 | 1.377078129 | 0.002094827 | 0.674070977 |
| <i>NA</i> | ENSG00000280374 | -1.908446479 | 0.002116105 | 0.674070977 |
| <i>PEXIIG</i> | ENSG00000104883 | -1.64352962 | 0.002517743 | 0.751817899 |
| <i>NA</i> | ENSG00000272841 | 2.085921021 | 0.00268939 | 0.76254564 |
| <i>NA</i> | ENSG00000267034 | 1.02179119 | 0.003073523 | 0.825372624 |
| <i>TRMT61A</i> | ENSG00000166166 | 1.230547487 | 0.003166882 | 0.825372624 |
| <i>NA</i> | ENSG00000226632 | 2.474821561 | 0.0033634 | 0.835385097 |
| <i>IFI27</i> | ENSG00000165949 | 2.654235993 | 0.003583636 | 0.855808299 |
| <i>KRT86*</i> | ENSG00000170442 | -3.099508734 | 0.003688596 | 0.855808299 |
| <i>PER3</i> | ENSG00000049246 | -1.008221097 | 0.00375306 | 0.856959661 |
| <i>SEMA3A</i> | ENSG00000075213 | 1.145874269 | 0.003971855 | 0.86848977 |
| <i>NA</i> | ENSG00000285554 | 2.392676774 | 0.004185527 | 0.878007923 |
| <i>NA</i> | ENSG00000225447 | -1.509240149 | 0.004280926 | 0.879560203 |
| <i>POLD4</i> | ENSG00000175482 | -1.111272808 | 0.004307395 | 0.879560203 |
| <i>CNIH3*</i> | ENSG00000143786 | -3.30000464 | 0.00454354 | 0.901787772 |
| <i>NA</i> | ENSG00000256393 | 1.678411723 | 0.005080971 | 0.966239624 |
| <i>FFAR2</i> | ENSG00000126262 | 1.07301739 | 0.005321545 | 0.966239624 |
| <i>TTC23</i> | ENSG00000103852 | 1.237361265 | 0.005742232 | 0.966239624 |
| <i>TNIP3</i> | ENSG00000050730 | 1.860231145 | 0.005759736 | 0.966239624 |
| <i>YPEL1</i> | ENSG00000100027 | -1.336695541 | 0.00649346 | 0.991386185 |
| <i>NA</i> | ENSG00000210164 | -1.165930877 | 0.00684723 | 0.997785732 |
| <i>WASH2P</i> | ENSG00000146556 | 1.537272136 | 0.00692405 | 0.997785732 |
| <i>ABHD17C</i> | ENSG00000136379 | 1.059222256 | 0.007425797 | 0.997785732 |
| <i>NA</i> | ENSG00000260317 | 1.454725355 | 0.00748741 | 0.997785732 |
| <i>IL1B</i> | ENSG00000125538 | 1.124032672 | 0.007627075 | 0.997785732 |
| <i>CCL8</i> | ENSG00000108700 | 1.456913088 | 0.007700658 | 0.997785732 |
| <i>TSPAN15</i> | ENSG00000099282 | -1.78059737 | 0.007787389 | 0.997785732 |
| <i>CSF1</i> | ENSG00000184371 | -1.311989813 | 0.00811142 | 0.997785732 |
| <i>RAVER2</i> | ENSG00000162437 | 3.81308529 | 0.008155484 | 0.997785732 |

| | | | | |
|---------------------|-----------------|--------------|-------------|-------------|
| <i>ITGB8</i> | ENSG00000105855 | 1.383004583 | 0.008239489 | 0.997785732 |
| <i>NA</i> | ENSG00000262979 | 1.891203212 | 0.008905453 | 0.997785732 |
| <i>NA</i> | ENSG00000275769 | -3.039747183 | 0.009122883 | 0.997785732 |
| <i>NA</i> | ENSG00000261618 | 2.738691309 | 0.009399018 | 0.997785732 |
| <i>CESI</i> | ENSG00000198848 | -1.351234248 | 0.00960455 | 0.997785732 |
| <i>TRGC2</i> | ENSG00000227191 | 1.87219908 | 0.009757642 | 0.997785732 |
| <i>NA</i> | ENSG00000279502 | -2.358142683 | 0.009798447 | 0.997785732 |
| <i>ZNF79</i> | ENSG00000196152 | -1.257711983 | 0.009855672 | 0.997785732 |
| <i>FCRL1</i> | ENSG00000163534 | 1.829359047 | 0.009868655 | 0.997785732 |
| <i>STN1</i> | ENSG00000107960 | -1.059537111 | 0.009956252 | 0.997785732 |

8.4.2. Visualization and Functional Interpreting of DEGs

The prospective molecular and biological mechanisms involved in the pathogenesis of ASD were decoded, subjecting significant DEGs to GO and KEGG analysis. As demonstrated in **(Figure 8.2A)**, the GO analysis revealed that numerous BP in ASD brain datasets were prominently involved in the positive regulation of cytokine production, response to molecules of bacterial origin, and response to lipopolysaccharide. The key MF enriched by the DEGs encompassed receptor ligand activity and DNA-binding transcription activator activity, as depicted in **Figure 8.2B**. However, the DEGs primarily encoded the cellular components known as collagen-containing extracellular matrix and secretory granule lumen **(Figure 8.2C)**. Furthermore, KEGG pathway enrichment analysis was accomplished for the nominally significant DEGs from the brain dataset; five pathways exhibited statistically meaningful enrichment with P -value < 0.01 . The top three pathways included the TNF signaling pathway, NF-kappa B signaling pathway, and Malaria, as visualized in **Figure 8.2D**.

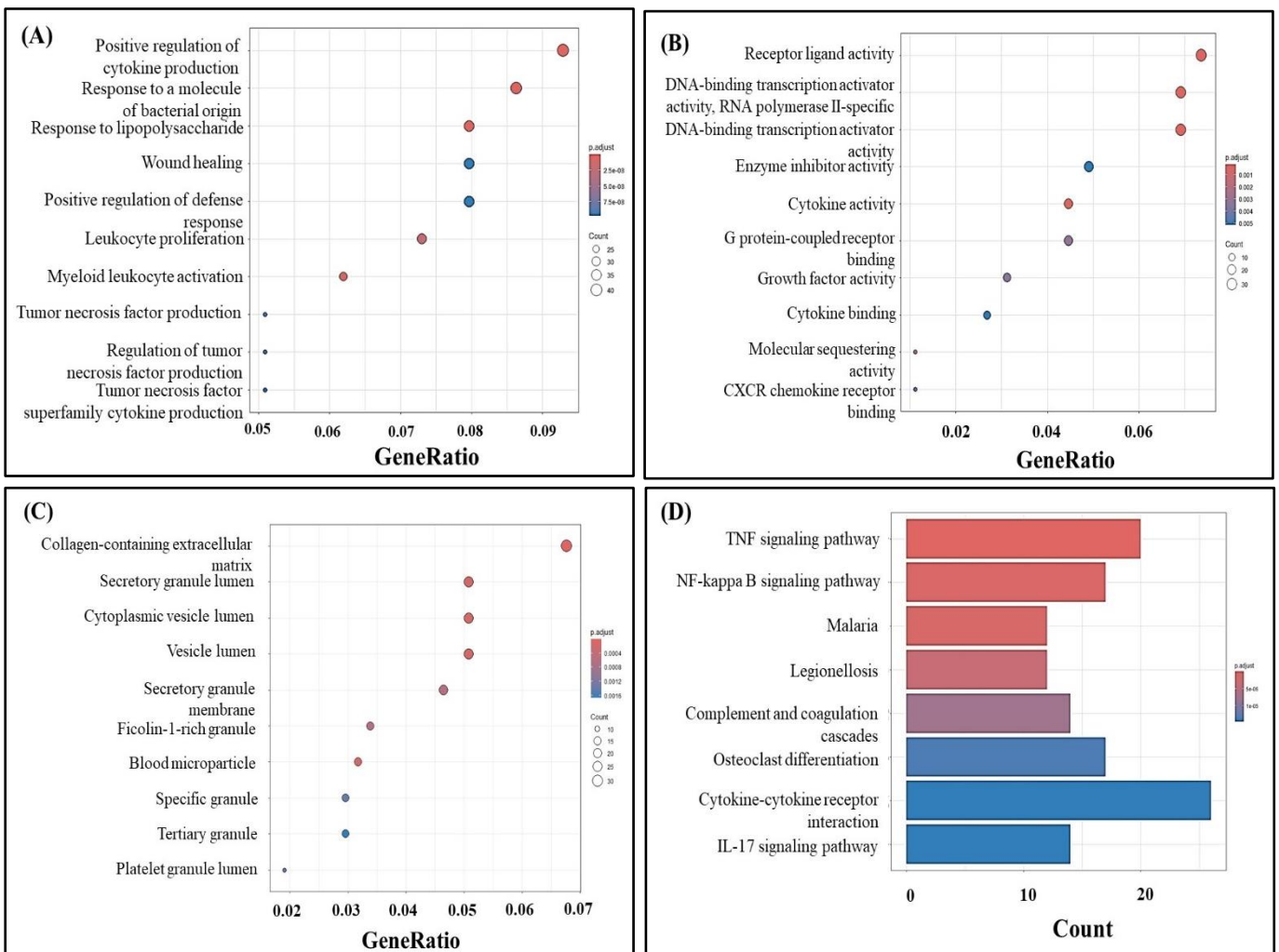


Figure 8.2. Enriched GO and KEGG analysis of brain dataset. (A) points to the biological process category, (B) to cellular components, and (C) to molecular function. The Padj-value (FDR) is used to color-code the bars ranging from blue to red, and (D) the bar plot represents the KEGG pathways enriched by DEGs. Based on the FDR, the bars are colored from blue to red.

In the same context, the KEGG pathways and GO terms engaged with the significant DEGs from the blood dataset were explored. The enriched BP related to the DEGs included leukocyte migration, granulocyte migration and leukocyte chemotaxis, as depicted in **Figure 8.3A**. In terms of MF, the DEGs list exhibited enrichment in receptor-ligand activity, cytokine activity, and cytokine receptor binding as illustrated in **Figure 8.3B**. In the context of the CC category, there was enrichment in the Cytokine-cytokine receptor interaction and viral protein interaction with cytokine and cytokine receptor.

The KEGG analysis findings of DEGs of blood showed notable enrichment pathways in cytokine-cytokine receptor interaction, chemokine signaling pathway, and viral protein interaction with cytokine and cytokine receptor (Figure 8.4).

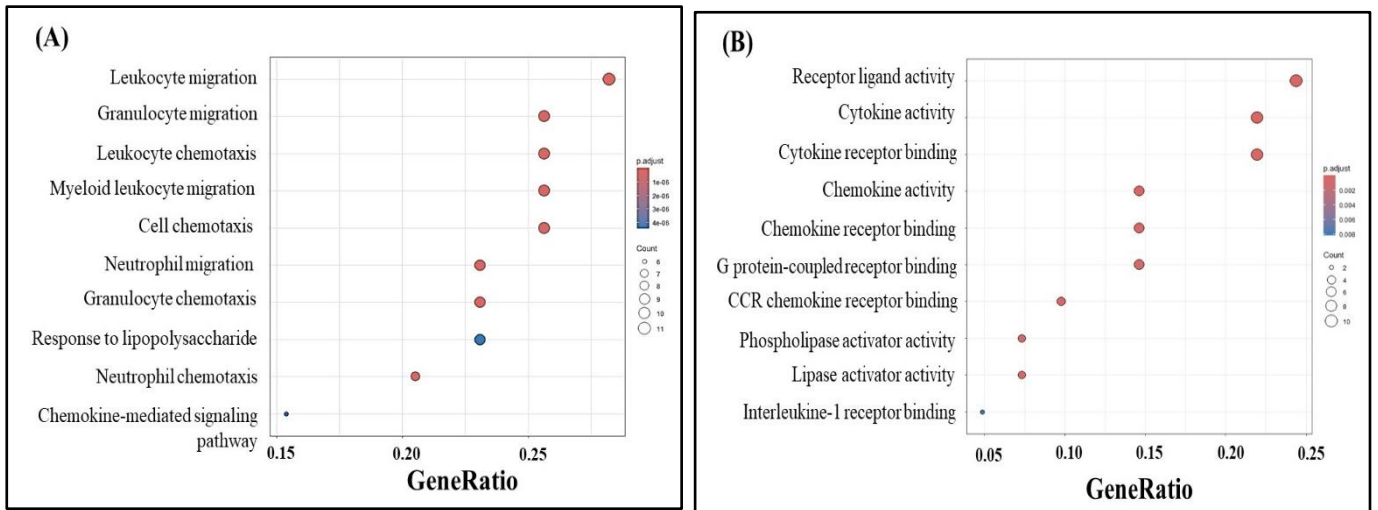


Figure 8.3. Enriched GO of the blood dataset. (A) points to the biological process category and (B) to molecular function. The FDR is used to color the dots, which range from blue to red, and the count of genes determines the size of the dots.

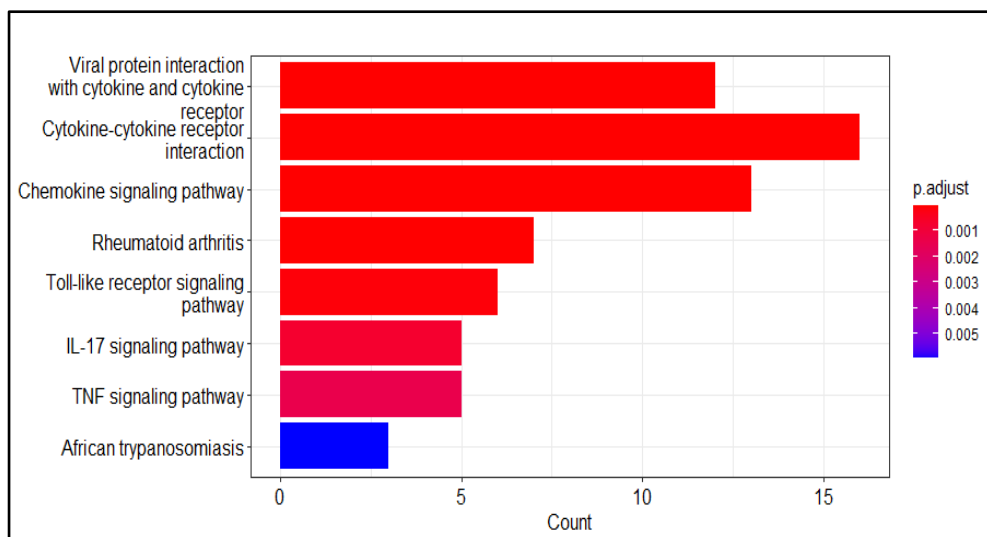


Figure 8.4. KEGG analysis of blood dataset. The bar plot depicts the KEGG pathways enriched by DEGs (P-value 0.01). The Padj- value determines the color of the bars, which range from blue to red.

8.4.3. Comparison DEGs between two datasets and Functional Annotation

The common genes identified in both datasets are presented in the Venn diagram (**Figure 8.5** and **Table 8.3**). A total of eight DEGs were discerned, potentially serving as pathogenic genes in ASD. Among these DEGs, *UPBI*, *CXCL1*, *CXCL10*, *CSF1*, *CCL2*, and *IL1B* demonstrated associations with previously detected ASD susceptibility genes. Intriguingly, no investigations have been conducted on these genes in the context of ASD within brain tissues. Notably, the remaining two genes (*FFAR2* and *WWC2-AS2*) are novel and have not been previously linked to ASD.

Based on the KEGG pathway analysis outcomes, the eight DEGs were predominantly enriched in the biological processes, including the TNF signaling pathway, cytokine-cytokine receptor interaction, and the IL-17 signaling pathway (**Table 8.4**).

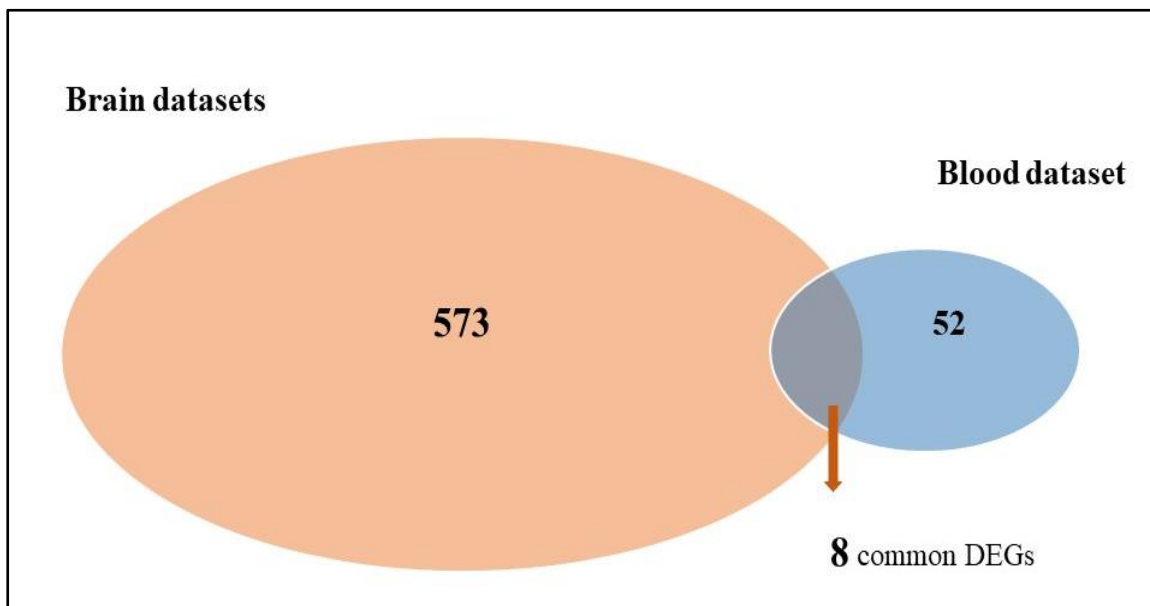


Figure 8.5. Venn map represents the eight common genes crossing among two datasets. The orange circle shows the 573 DEGs of the brain dataset; the blue circle shows the 52 DEGs of the blood dataset, considering P -value < 0.01 threshold for both, and the purple region shows eight common genes between the two datasets.

1 **Table 8.3.** Eight common genes are shared between the brain dataset and the blood dataset

| Gene Symbol | Entrez ID | Function | Remark | Ref. |
|---------------|-----------|---|--|----------|
| <i>UPBI</i> | 51733 | The enzyme β UP. Its role in the final step of pyrimidine breakdown produces two products, both of which are speculated to affect nervous system functions. | | [22] |
| <i>CXCL1</i> | 2919 | It is one of the CXC subgroups of chemokines and is capable of chemoattraction to neutrophils. | High-functioning ASD groups showed increased <i>CXCL1</i> plasma levels. | [23] |
| <i>CXCL10</i> | 3627 | <i>CXCL10</i> induces immune cells, like natural killer cells, macrophages, and dendritic cells. | <i>CXCL10</i> levels in autistic patients' Cerebrospinal fluid were elevated compared to controls. | [24] |
| <i>CCL2</i> | 6347 | Is a member of chemokines superfamily involved in immunoregulatory and inflammatory processes | Elevated levels of <i>CCL2</i> in ASD subjects | [25, 26] |

| | | | | |
|------------------------|--------|--|---|----------|
| <i>IL1B</i> | 3553 | <i>IL1 β</i> interacting protein is abundant in lymph nodes. | ASD samples have been linked to heightened levels of inflammatory cytokines, including IL-1β in biological fluids | [27, 28] |
| <i>CSF1</i> | 1435 | is a hematopoietic growth factor included in the reproduction, differentiation, and survival of monocytes, macrophages | Mechanism mediated by CSF1-CSF1R signaling contributes to sociable behavior and motor function. | [29] |
| <i>FFAR2</i> | 2867 | free fatty acid receptor | | |
| <i>WWC2-AS2</i> | 152641 | WWC2 Antisense Gene Protein 2 | | |

Table 8.4. Significant enriched KEGG of eight common genes.

| KEGG Pathways | Count | Genes | P-Value |
|--|-------|--|---------|
| TNF signaling pathway | 5 | <i>CCL2, CXCL10, CXCL1, CSF1, IL1B</i> | 4.2E-7 |
| Cytokine-cytokine receptor interaction | 5 | <i>CCL2, CXCL10, CXCL1, CSF1, IL1B</i> | 1.9E-5 |
| IL-17 signaling pathway | 4 | <i>CCL2, CXCL10, CXCL1, IL1B</i> | 2.4E-5 |
| Rheumatoid arthritis | 4 | <i>CCL2, CXCL1, CSF1, IL1B</i> | 2.4E-5 |

8.5. Discussion:

Early clinical prediction of ASD, together with targeted interventions, has been an area of interest, and several studies have been conducted to determine biomarkers with disease-predictive potential [6, 14, 15]. Nonetheless, the potent and accurate biomarkers for detecting and diagnosing ASD are an unmet challenge. In the present study, we have investigated the DEGs in the brain and blood tissues of ASD patients. The results of the brain datasets showed 581 DEGs. Of these, 520 genes were considered significantly expressed upregulated genes. The top three significant upregulated genes included immune response genes, namely, *HSPA6*, *CSF3*, and *SERPINA3*. *CSF3* gene encodes interleukin-6 (IL-6). The results obtained from children diagnosed with ASD revealed augmented production of IL-6 in lipopolysaccharide (LPS)-stimulated monocytes. Notably, this heightened IL-6 production exhibited a correlation with the manifestation of restricted and repetitive behaviors, thereby implicating an association between excessive inflammation stemming from innate immune responses and aberrant behavioral patterns in ASD [19, 30]. Choi et al. [31] pointed out that the production of IL-17 in maternal inflammation induces IL-6, interfering with fetal neurological development and causing ASD. Previous papers have suggested a link between IL-6 and ASD. Nevertheless, the precise nature of this relationship and its role in ASD pathogenesis are still areas of active investigation. Furthermore, *HSPA6* was unveiled to be a dysregulated gene correlated with microglia in the post-mortem brains of neuropsychiatric patients [32]. Similarly, comparative transcriptome investigation highlighted *HSPA6* as a significant upregulation gene related to immune system dysregulation in ASD subjects [33]. Prior research has documented heightened levels of *SERPINA3* and proinflammatory cytokines in the cerebral regions of individuals with schizophrenia [34]. Furthermore, *SERPINA3* and heat shock proteins have been linked to

neuroinflammation [35]. Conversely, mice with a knock-in of *SERPINA3* demonstrated improved cognitive capacities in behavioral tasks. Notably, the upregulation of *SERPINA3* resulted in increased neocortical folding, augmented neuronal abundance, and improved cognitive performance [36]. Conversely, the *TRAVI-1* gene, which was among the downregulated genes, encodes an alpha chain in the V region of the T cell receptor variable domain that participates in antigen recognition. T cells play roles in dysregulation immunity in ASD subjects [37].

The meta-analysis of the blood dataset revealed 60 DEGs. *RAVER2* gene was the highest upregulated, whereas *CNIH3* and *TRIB3* were downregulated significant DEGs. *CNIH3* is a member of the cornichon family of transmembrane proteins that play a role in the regulation of α -amino-3-hydroxyl-5-methyl-4-isoxazole-propionate (AMPA) receptor [38]. *CNIH3* is involved in synaptic plasticity, learning, and memory [39]. Cheng et al. [40] reported that alterations or deficits in AMPAR lead to specific neurological disorders like ASD and epilepsy. Our findings align with previously mentioned studies [40, 41], indicating that *CNIH3* could be used as a susceptible gene linked to ASD. However, further research is needed to fully understand the role of *CNIH3* and its potential as a therapeutic target for neurological disorders.

Zhang et al. [42] noticed that higher levels of the *TRIB3* gene could inhibit kainic acid (KA), which is known to cause neuronal apoptosis and seizures. Meanwhile, lower levels of *TRIB3* have been shown to protect against KA-induced neuronal apoptosis, leading to the conclusion that *TRIB3* could be a promising therapeutic target for epilepsy recovery. Conversely, in the current study, *TRIB3* was downregulated in ASD patients. Therefore, further investigations are needed to understand the molecular function of *TRIB3* in ASD, especially considering reports that suggest approximately 21.5% of ASD patients also have epilepsy [43, 44].

RAVER2 is an RNA-binding protein [45]. The function of *RAVER2* in neurodevelopmental diseases is not well known because of its restricted transcription pattern and absence of expression in brain cell lines [46]. However, the gene-wise analysis revealed a genome-wide meaningful correlation between *RAVER2* and the capacity to recognize feelings in ASD patients [47]. A recent study has been applied to predict relevant risk genes associated with Parkinson's disease (PD) and revealed that

RAVER2 was an upregulated DEG [48]. Therefore, it shows that *RAVER2* may affect ASD pathogenesis; thus, more investigation is required to detect its biological pathways.

Functional and enrichment analysis of the brain dataset revealed the positive regulation of cytokine production and response to lipopolysaccharide. According to epidemiological statistics, maternal immune activation may contribute to the emergence of ASD [49, 50]. It is noteworthy that LPS, a Gram-negative bacteria cellular membrane constituent, can trigger a pro-inflammatory cascade, primarily through stimulated macrophage/microglial cells [51]. As a result, it evokes many modifications in the inflammatory responses, contributing to a detrimental influence on the maturation of synapses [52]. Numerous studies have documented that prenatal intake of LPS caused immunological dysfunction [53, 54] as well as behavioral dysfunctions in mice, including communicative difficulties, social deficits, and stereotypical behavior [55-57]. Taken together, chronic neuroinflammation emerges as a pivotal contributor to the development of ASD [58, 59] by causing an overproduction of proinflammatory cytokines, resulting in severe pathophysiological alterations and neurobehavioral issues [9, 60-62].

An enrichment analysis of the blood dataset showed significantly enriched pathways, including responses to chemokine and cytokine-cytokine receptor interaction pathways. The DEGs implicated in previous pathways were *CCL2*, *CCL23*, *CCL3*, *CXCL1*, and *CXCL10*. Case-control research from peripheral blood demonstrated that the concentration of *CCL2* was significantly high in ASD children [25]. Chen et al. [26] revealed significantly increased serum levels of *CCL3* in ASD model mice [63]. In the same context, *CCL5* has been linked to inflammatory responses in the brain [64]. Likewise, levels of *CCL2*, *CCL3*, and *CCL5* peripheral blood were observed to be higher in ASD samples [25, 26]. These chemokines have been implicated in a lack of attention and hyperactivity behaviors, neuroinflammation, and cerebral infarction [25, 65]. Consequently, these proteins might have a potential role in neuroinflammation and affect ASD pathogenesis.

The autism transcriptomic datasets in brain and blood cells are bound to vary; the expression of genes in blood might co-regulate with genes associated with central nervous system (CNS) pathogenesis, making them highly valuable biomarkers. However, transcriptomic adjustments in the brains of autistic subjects might be the most crucial components of CNS pathogenesis; nevertheless, they may not possess predictive value if

these genes are not expressed or modified in obtainable peripheral tissue. Consequently, our approach was to detect the common genes between the brain and the blood datasets as robust candidate biomarkers in ASD patients. The eight common genes were *UPBI*, *CXCL1*, *CXCL10*, *CSF1*, *IL1B*, *CCL2*, *FFAR2* and *WWC2-AS2*. A previous study assessed 60 growth factors and cytokines levels. They found an array of changes in interleukins and CXC chemokines, such as *CXCL10*, which indicates a dysregulated immune response in pregnant mothers and in the cord blood of newborns later diagnosed with ASD [66]. Vargas et al. [24] noticed an increase in the level of *CXCL10* in the CSF of the ASD group compared to the healthy controls. In the same context, Osborne et al. [67] indicated an increase in the *CXCL10* serum level due to early-life inflammatory responses, which could be potential reasons for autism disorder. In contrast, a previous study reported increased *CXCL1* plasma levels in high-functioning ASD groups [23].

On the other hand, the *UPBI* gene encodes a beta-ureidopropionase (β UP) enzyme, which is implied in the pyrimidine breakdown process' last stage. β UP enzyme transforms N-carbamyl-beta-aminoisobutyric acid into N-carbamyl-beta-alanine and beta-aminoisobutyric acid, which in turn broken down into beta-alanine, ammonia, and carbon dioxide. Both of the products are presumed to have functions in the nervous system. Beta-aminoisobutyric acid induces leptin protein production, which protects nerve cells from injury due to toxins, inflammatory processes, etc. [68]. Beta-alanine is engaged in signal pathways in neuronal synapses and controls the neurotransmitter dopamine level [69]. Dopamine influences the alteration of behavior, cognition, awareness, sleep, verbal memory, acquiring knowledge, inspiration, voluntary movement, and punishment and rewards [68]. Dichter et al. [70] highlighted the impact of dopamine deficits on the specific brain area and concluded that the impairments could cause autistic-like behavior. In the same context, individuals with β UP deficiency are diagnosed in the early years of life with clinical features such as verbal deficit, mental disabilities, growth failure, and seizures [22]. *CSF1* signaling has been shown to be necessary for the survival, migration, and activation of microglia in the cerebellum. Therefore, the deficiency of *CSF1* reduced the number of microglia in the cerebellum, leading to impaired motor function, learning, memory, and social interaction [29]. However, the molecular function of these genes and their roles in ASD pathogenesis are unknown well. *FFAR2*, as a free fatty acid receptor, plays a pivotal role in the regulation of the immune system by influencing the expansion, development, and function of T

cells as well as the local intestine dendritic cell population [71]. Additionally, *FFAR2* knockout mice lacking the short-chain fatty acid (SCFA) receptor, exhibited notable morphological, functional, and developmental modifications in microglial cells [72]. Currently, there is a lack of studies establishing a link between *FFAR2* and ASD. Further investigations are required.

The KEGG enrichment pathways of the common genes were implicated in the TNF signaling and cytokine-cytokine receptor interaction pathways, which aligned with the findings of prior studies, suggesting the linkage between these pathways and the development of ASD [13, 30].

8.6. Conclusion

In conclusion, the current study sought to identify high-risk genes in both brain and blood datasets from individuals with ASD. These DEGs caused a cascade of immune activation abnormalities, elevated cytokine production, and ultimately manifested in abnormal alterations in molecular signaling pathways and neuronal synapses, potentially contributing to the pathogenesis of ASD. However, further experimental validation is essential to elucidate the biological functions of these DEGs in the pathophysiology of ASD. Meanwhile, our approach identified eight common genes, suggesting these genes can be potential biomarkers for the early detection of ASD from available tissues and represent prospective targets for future pharmacological interventions in ASD. Nevertheless, extensive research with larger sample sizes is warranted to validate these findings and enable accurate early diagnosis of ASD.

References:

- [1] Zeidan, J., Fombonne, E., Scolah, J., Ibrahim, A., Durkin, M. S., Saxena, S., Yusuf, A., Shih, A. and Elsabbagh, M. Global prevalence of autism: A systematic review update. *Autism research*, 15: 778-790, 2022. <https://doi.org/10.1002/aur.2696>
- [2] Lipkin, W. I., Bresnahan, M. and Susser, E. Cohort-guided insights into gene–environment interactions in autism spectrum disorders. *Nat. Rev. Neurol.*, 19: 118–125, 2023. <https://doi.org/10.1038/s41582-022-00764-0>
- [3] Schaevitz, L. R. and Berger-Sweeney, J. E. Gene–environment interactions and epigenetic pathways in autism: the importance of one-carbon metabolism. *ILAR journal*, 53: 322-340, 2012. <https://doi.org/10.1093/ilar.53.3-4.322>

- [4] Sandin, S., Lichtenstein, P., Kuja-Halkola, R., Larsson, H., Hultman, C. M. and Reichenberg, A. The familial risk of autism. *Jama*, 311: 1770-1777, 2014. <https://doi:10.1001/jama.2014.4144>
- [5] Sun, Y., Yao, X., March, M. E., Meng, X., Li, J., Wei, Z., Sleiman, P. M., Hakonarson, H., Xia, Q. and Li, J. Target genes of autism risk loci in brain frontal cortex. *Front. Genet.*, 10: 1-8, 2019. <https://doi.org/10.3389/fgene.2019.00707>
- [6] Wang, Y., Kou, Y. and Meng, D. Network structure analysis identifying key genes of autism and its mechanism. *Comput. Math. Methods Med.*, 2020: 1-9, 2020. <https://doi.org/10.1155/2020/3753080>
- [7] Satterstrom, F. K., Kosmicki, J. A., Wang, J., Breen, M. S., De Rubeis, S., An, J.-Y., Peng, M., Collins, R., Grove, J. and Klei, L. Large-scale exome sequencing study implicates both developmental and functional changes in the neurobiology of autism. *Cell*, 180: 568-584, 2020. <https://doi.org/10.1016/j.cell.2019.12.036>
- [8] Matta, S. M., Hill-Yardin, E. L. and Crack, P. J. J. The influence of neuroinflammation in Autism Spectrum Disorder. *Brain, Behavior, and Immunity*, 79: 75-90, 2019. <https://doi.org/10.1016/j.bbi.2019.04.037>
- [9] Hughes, H., Moreno, R. and Ashwood, P. J. Innate immune dysfunction and neuroinflammation in autism spectrum disorder (ASD). *Brain, Behavior, and Immunity*, 108: 245-254, 2023. <https://doi.org/10.1016/j.bbi.2022.12.001>
- [10] Molloy, C. J., Cooke, J., Gatford, N. J., Rivera-Olvera, A., Avazzadeh, S., Homberg, J. R., Grandjean, J., Fernandes, C., Shen, S. and Loth, E. Bridging the translational gap: what can synaptopathies tell us about autism? *Frontiers in Molecular Neuroscience*, 16: 1-20, 2023. <https://doi.org/10.3389/fnmol.2023.1191323>
- [11] Than, U. T. T., Nguyen, L. T., Nguyen, P. H., Nguyen, X.-H., Trinh, D. P., Hoang, D. H., Nguyen, P. A. T. and Dang, V. D. J. S. R. Inflammatory mediators drive neuroinflammation in autism spectrum disorder and cerebral palsy. 13: 22587, 2023. <https://doi.org/10.1038/s41598-023-49902-8>
- [12] Filosi, M., Kam-Thong, T., Essioux, L., Muglia, P., Trabetti, E., Spooren, W., Müller-Myshok, B. and Domenici, E. Transcriptome signatures from discordant sibling pairs reveal changes in peripheral blood immune cell composition in Autism Spectrum Disorder. *Transl. Psychiatry*, 10: 1-12, 2020. <https://doi.org/10.1038/s41398-020-0778-x>
- [13] Rahman, M. R., Petralia, M. C., Ciurleo, R., Bramanti, A., Fagone, P., Shahjaman, M., Wu, L., Sun, Y., Turanli, B. and Arga, K. Y. Comprehensive analysis of RNA-seq

gene expression profiling of brain transcriptomes reveals novel genes, regulators, and pathways in autism spectrum disorder. *Brain Sci.*, 10: 747-763, 2020. <https://doi.org/10.3390/brainsci10100747>

[14] Ravaei, A., Emanuele, M., Nazzaro, G., Fadiga, L. and Rubini, M. Placental DNA methylation profile as predicting marker for autism spectrum disorder (ASD). *Mol. Med.*, 29: 8, 2023. <https://doi.org/10.1186/s10020-022-00593-3>

[15] Lawrence, K. E., Hernandez, L. M., Fuster, E., Padgaonkar, N. T., Patterson, G., Jung, J., Okada, N. J., Lowe, J. K., Hoekstra, J. N. and Jack, A. Impact of autism genetic risk on brain connectivity: a mechanism for the female protective effect. *Brain*, 145: 378-387, 2022. <https://doi.org/10.1093/brain/awab204>

[16] Garrido-Torres, N., Guzmán-Torres, K., García-Cerro, S., Pinilla Bermúdez, G., Cruz-Baquero, C., Ochoa, H., García-González, D., Canal-Rivero, M., Crespo-Facorro, B. and Ruiz-Veguilla, M. miRNAs as biomarkers of autism spectrum disorder: a systematic review and meta-analysis. *Eur. Child Adolesc. Psychiatry*, 1-34, 2023. <https://doi.org/10.1007/s00787-023-02138-3>

[17] Zhu, Y., Gomez, J. A., Laufer, B. I., Mordaunt, C. E., Mouat, J. S., Soto, D. C., Dennis, M. Y., Benke, K. S., Bakulski, K. M. and Dou, J. Placental methylome reveals a 22q13. 33 brain regulatory gene locus associated with autism. *Genome Biol.*, 23: 46, 2022. <https://doi.org/10.1186/s13059-022-02613-1>

[18] Irimia, M., Weatheritt, R. J., Ellis, J. D., Parikshak, N. N., Gonatopoulos-Pournatzis, T., Babor, M., Quesnel-Vallières, M., Tapial, J., Raj, B. and O'Hanlon, D. A highly conserved program of neuronal microexons is misregulated in autistic brains. *Cell*, 159: 1511-1523, 2014. <https://doi.org/10.1016/j.cell.2014.11.035>

[19] Hughes, H. K., Rowland, M. E., Onore, C. E., Rogers, S., Ciernia, A. V. and Ashwood, P. Dysregulated gene expression associated with inflammatory and translation pathways in activated monocytes from children with autism spectrum disorder. *Transl. Psychiatry*, 12: 1-9, 2022. <https://doi.org/10.1038/s41398-021-01766-0>

[20] Love, M., Anders, S. and Huber, W. Differential analysis of count data—the DESeq2 package. *Genome Biol.*, 15: 10-1186, 2014. <https://doi.org/10.1186/s13059-014-0550-8>

[21] Wu, T., Hu, E., Xu, S., Chen, M., Guo, P., Dai, Z., Feng, T., Zhou, L., Tang, W. and Zhan, L. clusterProfiler 4.0: A universal enrichment tool for interpreting omics data. *Innovation*, 2: 100141, 2021. <https://doi.org/10.1016/j.xinn.2021.100141>

- [22] Dobritzsch, D., Meijer, J., Meinsma, R., Maurer, D., Monavari, A. A., Gummesson, A., Reims, A., Cayuela, J. A., Kuklina, N. and Benoist, J.-F. β -Ureidopropionase deficiency due to novel and rare UPB1 mutations affecting pre-mRNA splicing and protein structural integrity and catalytic activity. *Mol. Genet. Metab.*, 136: 177-185, 2022. <https://doi.org/10.1016/j.ymgme.2022.01.102>
- [23] Suzuki, K., Matsuzaki, H., Iwata, K., Kamenon, Y., Shimmura, C., Kawai, S., Yoshihara, Y., Wakuda, T., Takebayashi, K. and Takagai, S. Plasma cytokine profiles in subjects with high-functioning autism spectrum disorders. *PloS one*, 6: e20470, 2011. <https://doi.org/10.1371/journal.pone.0020470>
- [24] Vargas, D. L., Nascimbene, C., Krishnan, C., Zimmerman, A. W. and Pardo, C. A. Neuroglial activation and neuroinflammation in the brain of patients with autism. *Annals of Neurology: Official Journal of the American Neurological Association the Child Neurology Society*, 57: 67-81, 2005. <https://doi.org/10.1002/ana.20315>
- [25] Han, Y. M., Cheung, W. K., Wong, C. K., Sze, S. L., Cheng, T. W., Yeung, M. K. and Chan, A. S. Distinct cytokine and chemokine profiles in autism spectrum disorders. *Front. Immunol.*, 8: 1-12, 2017. <https://doi.org/10.3389/fimmu.2017.00011>
- [26] Chen, K., Fu, Y., Wang, Y., Liao, L., Xu, H., Zhang, A., Zhang, J., Fan, L., Ren, J. and Fang, B. Therapeutic Effects of the In Vitro Cultured Human Gut Microbiota as Transplants on Altering Gut Microbiota and Improving Symptoms Associated with Autism Spectrum Disorder. *Microb. Ecol.*, 80: 475-486, 2020. <https://doi.org/10.1007/s00248-020-01494-w>
- [27] Chauhan, A., Sahu, J. K., Jaiswal, N., Kumar, K., Agarwal, A., Kaur, J., Singh, S. and Singh, M. Prevalence of autism spectrum disorder in Indian children: A systematic review and meta-analysis. *Neurology India*, 67: 100-104, 2019. <https://doi.org/10.4103/0028-3886.253970>
- [28] Ricci, S., Businaro, R., Ippoliti, F., Lo Vasco, V. R., Massoni, F., Onofri, E., Troili, G., Pontecorvi, V., Morelli, M. and Rapp Ricciardi, M. Altered cytokine and BDNF levels in autism spectrum disorder. *Neurotoxicity research*, 24: 491-501, 2013. <https://doi.org/10.1007/s12640-013-9393-4>
- [29] Kana, V., Desland, F. A., Casanova-Acebes, M., Ayata, P., Badimon, A., Nabel, E., Yamamuro, K., Sneebor, M., Tan, I.-L. and Flanigan, M. E. CSF-1 controls cerebellar microglia and is required for motor function and social interaction. *J. Exp. Med.*, 216: 2265-2281, 2019. <https://doi.org/10.1084/jem.20182037>

- [30] Hughes, H. K., Rowland, M. E., Onore, C. E., Rogers, S., Ciernia, A. V. and Ashwood, P. Dysregulated gene expression associated with inflammatory and translation pathways in activated monocytes from children with autism spectrum disorder. *Transl. Psychiatry*, 12: 39, 2022. <https://doi.org/10.1038/s41398-021-01766-0>
- [31] Choi, G. B., Yim, Y. S., Wong, H., Kim, S., Kim, H., Kim, S. V., Hoeffler, C. A., Littman, D. R. and Huh, J. R. The maternal interleukin-17a pathway in mice promotes autism-like phenotypes in offspring. *Science*, 351: 933-939, 2016. <https://DOI:10.1126/science.aad0314>
- [32] Sadeghi, I., Gispert, J. D., Palumbo, E., Muñoz-Aguirre, M., Wucher, V., D'Argenio, V., Santpere, G., Navarro, A., Guigo, R. and Vilor-Tejedor, N. Brain transcriptomic profiling reveals common alterations across neurodegenerative and psychiatric disorders. *Computational Structural Biotechnology Journal*, 2022. <https://doi.org/10.1016/j.csbj.2022.08.037>
- [33] Garbett, K., Ebert, P. J., Mitchell, A., Lintas, C., Manzi, B., Mirnics, K. and Persico, A. M. Immune transcriptome alterations in the temporal cortex of subjects with autism. *Neurobiol. Dis.*, 30: 303-311, 2008. <https://doi.org/10.1016/j.nbd.2008.01.012>
- [34] Saetre, P., Emilsson, L., Axelsson, E., Kreuger, J., Lindholm, E. and Jazin, E. Inflammation-related genes up-regulated in schizophrenia brains. *BMC Psychiatry*, 7: 1-10, 2007. <https://doi.org/10.1186/1471-244X-7-46>
- [35] Sanfilippo, C., Malaguarnera, L. and Di Rosa, M. Chitinase expression in Alzheimer's disease and non-demented brains regions. *Journal of the neurological sciences*, 369: 242-249, 2016. <https://doi.org/10.1016/j.jns.2016.08.029>
- [36] Zhao, J., Feng, C., Wang, W., Su, L. and Jiao, J. Human SERPINA3 induces neocortical folding and improves cognitive ability in mice. *Cell discovery*, 8: 124, 2022. <https://doi.org/10.1038/s41421-022-00469-0>
- [37] Rose, D. R., Yang, H., Careaga, M., Angkustsiri, K., Van de Water, J. and Ashwood, P. J. T cell populations in children with autism spectrum disorder and comorbid gastrointestinal symptoms. *Brain, Behavior, Immunity-Health*, 2: 100042, 2020. <https://doi.org/10.1016/j.bbih.2020.100042>
- [38] Rogawski, M. A. Revisiting AMPA receptors as an antiepileptic drug target: revisiting AMPA receptors as an antiepileptic drug target. *Epilepsy Curr.*, 11: 56-63, 2011. <https://doi.org/10.5698/1535-7511-11.2.56>

- [39] Schwenk, J., Harmel, N., Zolles, G., Bildl, W., Kulik, A., Heimrich, B., Chisaka, O., Jonas, P., Schulte, U. and Fakler, B. Functional proteomics identify cornichon proteins as auxiliary subunits of AMPA receptors. *Science*, 323: 1313-1319, 2009. <https://doi:10.1126/science.1167852>
- [40] Cheng, J., Dong, J., Cui, Y., Wang, L., Wu, B. and Zhang, C. Interacting partners of AMPA-type glutamate receptors. *J. Mol. Neurosci.*, 48: 441-447, 2012. <https://doi.org/10.1007/s12031-012-9724-6>
- [41] Herring, B. E., Shi, Y., Suh, Y. H., Zheng, C.-Y., Blankenship, S. M., Roche, K. W. and Nicoll, R. A. Cornichon proteins determine the subunit composition of synaptic AMPA receptors. *Neuron*, 77: 1083-1096, 2013. <https://doi.org/10.1016/j.neuron.2013.01.017>
- [42] Zhang, J., Han, Y., Zhao, Y., Li, Q., Jin, H. and Qin, J. Inhibition of TRIB3 protects against neurotoxic injury induced by kainic acid in rats. *Front. Pharmacol.*, 10: 1-10, 2019. <https://doi.org/10.3389/fphar.2019.00585>
- [43] Besag, F. M. Current controversies in the relationships between autism and epilepsy. *Epilepsy Behav.*, 47: 143-146, 2015. <https://doi.org/10.1016/j.yebeh.2015.05.032>
- [44] Peng, J., Zhou, Y. and Wang, K. Multiplex gene and phenotype network to characterize shared genetic pathways of epilepsy and autism. *Sci. Rep.*, 11: 1-16, 2021. <https://doi.org/10.1038/s41598-020-78654-y>
- [45] Romanelli, M. G., Lorenzi, P., Diani, E., Filippello, A., Avesani, F. and Morandi, C. Transcriptional regulation of the human Raver2 ribonucleoprotein gene. *Gene*, 493: 243-252, 2012. <https://doi.org/10.1016/j.gene.2011.11.036>
- [46] Brečević, L., Rinčić, M., Krsnik, Ž., Sedmak, G., Hamid, A. B., Kosyakova, N., Galić, I., Liehr, T. and Borovečki, F. Association of new deletion/duplication region at chromosome 1p21 with intellectual disability, severe speech deficit and autism spectrum disorder-like behavior: an all-in approach to solving the DPYD enigma. *Transl. Neurosci.*, 6: 59-86, 2015. <https://doi.org/10.1515/tnsci-2015-0007>
- [47] Corominas, R., Yang, X., Lin, G. N., Kang, S., Shen, Y., Ghamsari, L., Broly, M., Rodriguez, M., Tam, S. and Trigg, S. A. Protein interaction network of alternatively spliced isoforms from brain links genetic risk factors for autism. *Nat. Commun.*, 5: 1-12, 2014. <https://doi.org/10.1038/ncomms4650>

- [48] Vastrad, B. and Vastrad, C. Bioinformatics and next generation sequencing data analysis to identify key genes and pathways influencing in Parkinson's disease. *bioRxiv*, 1-109, 2022. <https://doi.org/10.1101/2022.02.27.482208>
- [49] Jash, S. and Sharma, S. Pathogenic infections during pregnancy and the consequences for fetal brain development. *Pathogens*, 11: 1-12, 2022. <https://doi.org/10.3390/pathogens11020193>
- [50] Solek, C. M., Farooqi, N., Verly, M., Lim, T. K. and Ruthazer, E. S. Maternal immune activation in neurodevelopmental disorders. *Developmental Dynamics*, 247: 588-619, 2018. <https://doi.org/10.1002/dvdy.24612>
- [51] Płóciennikowska, A., Hromada-Judycka, A., Borzęcka, K. and Kwiatkowska, K. Co-operation of TLR4 and raft proteins in LPS-induced pro-inflammatory signaling. *Cellular molecular life sciences*, 72: 557-581, 2015. <https://doi.org/10.1007/s00018-014-1762-5>
- [52] Carbone, E., Manduca, A., Cacchione, C., Vicari, S. and Trezza, V. Healing autism spectrum disorder with cannabinoids: A neuroinflammatory story. *Neuroscience Biobehavioral Reviews*, 121: 128-143, 2021. <https://doi.org/10.1016/j.neubiorev.2020.12.009>
- [53] Kirsten, T. B., Lippi, L. L., Bevilacqua, E. and Bernardi, M. M. LPS exposure increases maternal corticosterone levels, causes placental injury and increases IL-1 β levels in adult rat offspring: relevance to autism. *PloS one*, 8: e82244, 2013. <https://doi.org/10.1371/journal.pone.0082244>
- [54] Solmaz, V., Tekatas, A., Erdoğan, M. A. and Erbaş, O. Exenatide, a GLP-1 analog, has healing effects on LPS-induced autism model: inflammation, oxidative stress, gliosis, cerebral GABA, and serotonin interactions. *International Journal of Developmental Neuroscience*, 80: 601-612, 2020. <https://doi.org/10.1002/jdn.10056>
- [55] de Cossío, L. F., Guzmán, A., Van Der Veldt, S. and Luheshi, G. N. J. Prenatal infection leads to ASD-like behavior and altered synaptic pruning in the mouse offspring. *Brain, Behavior, and Immunity* 63: 88-98, 2017. <https://doi.org/10.1016/j.bbi.2016.09.028>
- [56] Kirsten, T. B. and Bernardi, M. M. Prenatal lipopolysaccharide induces hypothalamic dopaminergic hypoactivity and autistic-like behaviors: Repetitive self-grooming and stereotypies. *Behavioural brain research*, 331: 25-29, 2017. <https://doi.org/10.1016/j.bbr.2017.05.013>

- [57] Carbone, E., Buzzelli, V., Manduca, A., Leone, S., Rava, A. and Trezza, V. Maternal Immune Activation Induced by Prenatal Lipopolysaccharide Exposure Leads to Long-Lasting Autistic-like Social, Cognitive and Immune Alterations in Male Wistar Rats. *International Journal of Molecular Sciences*, 24: 3920, 2023. <https://doi.org/10.3390/ijms24043920>
- [58] Jiang, C.-C., Lin, L.-S., Long, S., Ke, X.-Y., Fukunaga, K., Lu, Y.-M. and Han, F. Signalling pathways in autism spectrum disorder: mechanisms and therapeutic implications. *Signal Transduction Targeted Therapy*, 7: 229, 2022. <https://doi.org/10.1038/s41392-022-01081-0>
- [59] Norden, D. M. and Godbout, J. Microglia of the aged brain: primed to be activated and resistant to regulation. *Neuropathology applied neurobiology*, 39: 19-34, 2013. <https://doi.org/10.1111/j.1365-2990.2012.01306.x>
- [60] Zhao, H., Zhang, H., Liu, S., Luo, W., Jiang, Y. and Gao, J. Association of peripheral blood levels of cytokines with autism spectrum disorder: a meta-analysis. *Front. Psychiatry*, 12: 1-13, 2021. <https://doi.org/10.3389/fpsy.2021.670200>
- [61] Kutuk, M. O., Tufan, E., Gokcen, C., Kilicaslan, F., Karadag, M., Mutluer, T., Yektas, C., Coban, N., Kandemir, H. and Buber, A. Cytokine expression profiles in Autism spectrum disorder: A multi-center study from Turkey. *Cytokine*, 133: 155152, 2020. <https://doi.org/10.1016/j.cyto.2020.155152>
- [62] Maric, D. M., Vojvodic, D., Maric, D. L., Velikic, G., Radomir, M., Sokolovac, I., Stefik, D., Ivkovic, N., Susnjevic, S. and Puletic, M. Cytokine Dynamics in Autism: Analysis of BMAC Therapy Outcomes. *International Journal of Molecular Sciences*, 24: 15080, 2023. <https://doi.org/10.3390/ijms242015080>
- [63] Shen, Y., Ou, J., Liu, M., Shi, L., Li, Y., Xiao, L., Dong, H., Zhang, F., Xia, K. and Zhao, J. Altered plasma levels of chemokines in autism and their association with social behaviors. *Psychiatry Res.*, 244: 300-305, 2016. <https://doi.org/10.1016/j.psychres.2016.07.057>
- [64] Jalosinski, M., Karolczak, K., Mazurek, A. and Glabinski, A. The effects of methylprednisolone and mitoxantrone on CCL5-induced migration of lymphocytes in multiple sclerosis. *Acta Neurol. Scand.*, 118: 120-125, 2008. <https://doi.org/10.1111/j.1600-0404.2008.00998.x>
- [65] Guo, Y. Q., Zheng, L. N., Wei, J. F., Hou, X. L., Yu, S. Z., Zhang, W. W. and Jing, J. M. Expression of CCL2 and CCR2 in the hippocampus and the interventional roles of

propofol in rat cerebral ischemia/reperfusion. *Exp. Ther. Med.*, 8: 657-661, 2014.

<https://doi.org/10.3892/etm.2014.1757>

[66] Che, X., Hornig, M., Bresnahan, M., Stoltenberg, C., Magnus, P., Surén, P., Mjaaland, S., Reichborn-Kjennerud, T., Susser, E. and Lipkin, W. I. Maternal mid-gestational and child cord blood immune signatures are strongly associated with offspring risk of ASD. *Mol. Psychiatry*, 27: 1527-1541, 2022.

<https://doi.org/10.1038/s41380-021-01415-4>

[67] Osborne, B. F., Turano, A., Caulfield, J. I. and Schwarz, J. M. Sex-and region-specific differences in microglia phenotype and characterization of the peripheral immune response following early-life infection in neonatal male and female rats. *Neurosci. Lett.*, 692: 1-9, 2019.

<https://doi.org/10.1016/j.neulet.2018.10.044>

[68] Schmitt, K. C., Rothman, R. B. and Reith, M. E. Nonclassical pharmacology of the dopamine transporter: atypical inhibitors, allosteric modulators, and partial substrates. *J. Pharmacol. Exp. Ther.*, 346: 2-10, 2013.

<https://doi.org/10.1124/jpet.111.191056>

[69] Ericson, M., Clarke, R. B., Chau, P., Adermark, L. and Söderpalm, B. β -Alanine elevates dopamine levels in the rat nucleus accumbens: antagonism by strychnine. *Amino acids*, 38: 1051-1055, 2010.

<https://doi.org/10.1007/s00726-009-0313-0>

[70] Dichter, G. S., Damiano, C. A. and Allen, J. A. Reward circuitry dysfunction in psychiatric and neurodevelopmental disorders and genetic syndromes: animal models and clinical findings. *J. Neurodev. Disord.*, 4: 1-43, 2012.

<https://doi.org/10.1186/1866-1955-4-19>

[71] Koh, A., De Vadder, F., Kovatcheva-Datchary, P. and Bäckhed, F. From dietary fiber to host physiology: short-chain fatty acids as key bacterial metabolites. *Cell*, 165: 1332-1345, 2016.

<http://dx.doi.org/10.1016/j.cell.2016.05.041>

[72] Erny, D., Hrabě de Angelis, A. L., Jaitin, D., Wieghofer, P., Staszewski, O., David, E., Keren-Shaul, H., Mahlakoiv, T., Jakobshagen, K. and Buch, T. Host microbiota constantly control maturation and function of microglia in the CNS. *Nature neuroscience*, 18: 965-977, 2015.

<https://doi.org/10.1038/nn.4030>